Global groundwater system archetypes identify predominant patterns in socioeconomic, ecological, and Earth system functions of groundwater

Xander Huggins[1,2,3]*, Tom Gleeson[1,4], Karen G. Villholth[5], Juan C. Rocha[6], James S. Famiglietti[7]

[1] Department of Civil Engineering, University of Victoria, Victoria, Canada
[2] Global Institute for Water Security, University of Saskatchewan, Saskatoon, Canada
[3] International Institute for Applied Systems Analysis, Laxenburg, Austria
[4] School of Earth and Ocean Sciences, University of Victoria, Victoria, Canada
[5] Water Cycle Innovation (Pty) Ltd., Bela-Bela, South Africa
[6] Stockholm Resilience Centre, Stockholm University, Stockholm, Sweden
[7] School of Sustainability, Arizona State University, Tempe, USA
* Corresponding author: xanderhuggins@uvic.ca

ORCIDs:

Xander Huggins:	0000-0002-6313-8299
Tom Gleeson:	0000-0001-9493-7707
Karen G. Villholth:	0000-0002-7552-6715
Juan C. Rocha:	0000-0003-2322-5459
James S. Famiglietti	0000-0002-6053-5379

Key points:

- Derives and maps 10 global groundwater archetypes based on Earth system, ecosystem, food system, and water management system functions
- All 37 major aquifers systems of the world are characterised by multiple archetypes
- Applies a two-stage self-organising map (SOM) methodology to derive archetypes

Abstract:

Groundwater is a dynamic component of the global water cycle that performs important social, economic, ecological, and Earth system functions. Identifying the patterns and relationships between groundwater's diverse functions can provide important insights to aid framework, model, and theory development on interactions between groundwater and its connected systems and can help generate context-appropriate management approaches to the global groundwater crisis. We harness the recent growth in global groundwater datasets and perform an archetyping analysis using sequenced self-organising maps to derive a novel typology of groundwater systems based on its diverse, large-scale system functions that include storage capacity, climate coupling, groundwater-dependent ecosystems, irrigation, and water management. Our results, a 5-arcminute (~10 km) global map of 10 clearly discernible groundwater system archetypes (GAs), present a data-driven, integrated typology of groundwater's large-scale socioeconomic, ecological, and Earth system functions. Each archetype represents a distinct configuration of functions that reoccur over broad spatial extents. We evaluate archetype distributions across the 37 large aquifer systems of the world. Some aquifers are dominated by only a few archetypes (e.g., the Amazon and Congo Basins) whereas others contain a complex mosaic of many archetypes (e.g., Song-Liao and Maranao Basins). Yet, every large aquifer system we analysed is characterised by multiple archetypes, highlighting the insufficiency of treating these groundwater systems as homogeneous units in global groundwater assessments, models, and management. This archetyping study offers a further step towards developing causal understandings of system behaviour in these dynamically intertwined, complex, large-scale systems connected to groundwater.

Keywords:

Groundwater systems, Archetypes, Social-ecological systems, Self-organising maps

- main text begins on next page -

1 Introduction

Groundwater systems perform and provide many social, economic, ecological, and Earth system functions (Gleeson et al. 2020; Shah et al. 2007; Foster et al. 2013). Growing awareness about diverse system connections with groundwater suggests that comprehensive approaches to understand groundwater system dynamics can only be realised when these connections are considered (Huggins et al. 2023). These system connections and their associated functions do not exist uniformly and instead are distributed heterogeneously around the world. Yet, no study to date has synthesised or identified patterns in groundwater's multiple social, economic, ecological, and Earth system functions over the global domain.

Given the dominant influence humans exert on the global water cycle (Abbott et al. 2019), groundwater systems are undergoing rapid change under myriad human-mediated pressures. These pressures are exemplified by the rate of global groundwater depletion having doubled since the 1960-2000 time period (Döll et al. 2014), the prevalence of potential groundwater pumping-induced land subsidence across major mid-latitude aquifers (Herrera-García et al. 2021), the global extent of land use change (Winkler et al. 2021), and the exacerbating effect of climate change on groundwater resources (Taylor et al. 2013). These pressures articulate the global groundwater crisis (Famiglietti 2014), which is realised through impacts across systems connected to groundwater (Aeschbach-Hertig and Gleeson 2012; Foster and Chilton 2003). These include water security impacts, such as one in five wells globally being at risk of running dry (Jasechko and Perrone 2021), food security impacts such as over 25% of global food crop calories being grown in stressed and drying basins where groundwater depletion is prevalent (Huggins et al. 2022), and ecological impacts such as the potential for up to 80% of watersheds with current groundwater pumping to exceed environmental flow thresholds by 2050 (de Graaf et al. 2019).

Groundwater systems have been evaluated and mapped globally on the basis of their physical attributes, such as through the World-wide Hydrogeological Mapping and Assessment Programme (WHYMAP) (Richts et al. 2011), and for individual system interactions with groundwater, such as groundwater-climate interactions (Cuthbert et al. 2019), groundwater-ecological interactions (Fan et al. 2017), and food system interactions with groundwater including global virtual water trade networks (Dalin et al. 2017) and irrigation areas (Siebert et al. 2010). Yet, patterns in these diverse socioeconomic, ecological, and Earth system functions remain to be investigated by any integrated study. Doing so would enable the identification of common patterns across these functions that could help define, understand, and manage integrated groundwater systems across global contexts and through the various human-mediated pressures outlined above. We view this as an important direction for large-scale groundwater science, with the ambition of confronting deep knowledge gaps and epistemic uncertainties regarding groundwater system interactions across multiple dynamically connected systems and geographic scales.

System classification to understand drivers of hydrological system behaviour is commonplace in hydrological research and has been performed through conceptual (such as the hydrologic landscapes of Winter 2001) and data-driven approaches (such as clustering of catchment attributes, e.g, Jehn et al. 2020; Reinecke et al. 2019). However, classification studies that explicitly integrate socioeconomic, ecological, and Earth system components are rare and focus only on single system interactions with groundwater rather than using comprehensive, social-ecological system approaches. For example, Shah et al. (2007) developed a typology of groundwater economies at the nation scale but did not consider other groundwater functions. Existing classification schemes are important building blocks to develop a comprehensive understanding of groundwater systems and their behaviour, and expanding these efforts to include people, economies, ecosystems, and the Earth system in a holistic manner is a necessary development in large-scale groundwater science to further empower the science to assist and facilitate physical sustainability, social well-being, environmental justice, ecological integrity, and Earth system resilience (Sivapalan et al. 2014; Mukherji and Shah 2005; Abbott et al. 2019; Gleeson et al. 2020; Curran et al. 2023).

Inspired by other initiatives to “put people in the map” (Ellis and Ramankutty 2008), we attempt to disentangle the interactions between groundwater and its connected social-ecological systems, globally, by developing a classification map that explicitly includes interactions between groundwater, human activity, ecosystems, and the Earth system. To accomplish this, we turn to archetyping analysis, a growing pursuit in sustainability science that seeks to develop social-ecological system typologies to investigate phenomena of interest, develop theories of change within integrated human-environmental systems, and support sustainability goals (Eisenack et al. 2021). Social-ecological systems are integrated systems formed by the dynamic interactions between society and biophysical systems (Berkes and Folke 1998), and archetyping seeks to identify recurrent patterns in the attributes or behaviours of these systems (Sietz et al. 2019; Oberlack et al. 2019). Thus, archetyping groundwater systems can facilitate an integrated understanding of groundwater systems that existing classification schemes either miss or only partially address. Archetyping studies have been performed across global to local scales and individual studies are often conducted at a single scale (Sietz et al. 2019). Archetyping has been applied across a wide range of topics (Oberlack et al. 2023; Eisenack et al. 2021; Sietz et al. 2019). At the global scale, these studies include archetypes of land systems (Václavík et al. 2013), dryland vulnerability patterns (Sietz et al. 2011; Kok et al. 2016), functional regions of agricultural lands (Fridman et al. 2021), and deforestation frontiers of tropical dry woodlands (Buchadas et al. 2022). To our knowledge, formal archetyping analysis has yet to be explicitly applied to groundwater systems.

Here, we present the first archetyping study of groundwater systems at the global scale based on groundwater's Earth system, ecosystem, food system, and water management system functions, each documented by existing global datasets. We developed our groundwater archetypes using a sequenced, two-stage self-organising map (SOM), which represents the first application of this approach in the archetyping literature. Our motivation is to explore the heterogeneity in the intertwined, large-scale functions of groundwater and to classify predominant patterns. This classification can serve as a starting-point to aid in developing causal understandings of complex system behaviour in these deeply intertwined, large-scale systems. Recognizing the limits of current data quality and availability, we provide these archetypes as a baseline for future refinement, including the development of dynamic and outcome-specific archetypes. The archetypes also provide insights regarding impacts likely to be experienced from groundwater trends such as depletion, interannual variability, and quality degradation. Thus, archetypes can be equally important and useful for groundwater sustainability and management purposes. This study focuses on the methodology development, derivation, and description of the groundwater system archetypes, while management and sustainability implications are left for a follow-on study.

2 Materials and methods

2.1 Conceptual model

Our conceptual model is based on the recently developed groundwater-connected systems framing (Huggins et al. 2023) which centres the view of groundwater systems as embedded within social-ecological systems. The framing draws heavily on the Social-Ecological Systems Framework (Ostrom 2009) and places equal focus on groundwater's biophysical and social system interactions. Drawing on recent reviews of global groundwater resources (Gleeson et al.

2020; Lall et al. 2020; Scanlon et al. 2023), we identified four core systems that interact with groundwater across broad spatial scales and balance representation of groundwater's biophysical (B) and socioeconomic (S) functions: Earth systems (B), ecosystems (B), food systems (S), and water management systems (S) (Figure 1).

In the paragraphs below, we outline our selection process of the system functions used in our archetyping analysis. For each system, we selected two core functions of the identified system and its interactions with groundwater and each function is represented by an existing global dataset. These data inputs were determined based on our conceptual framing of large-scale groundwater functions, existing data availability, and an objective to balance the number of input datasets evenly across the four systems considered. Whereas previous archetyping studies use considerably more input datasets ($n \gg 8$, such as in Václavík et al. (2013) and Rocha et al. (2020)), it is increasingly encouraged to construct archetypes based on data inputs with strong conceptual links to the study's framing which often reduces the number of datasets used (Piemontese et al. 2022).

For groundwater's *Earth system* functions, we focus on climate and storage. Water table depth is an important control on the land-atmosphere energy balance (Maxwell and Kollet 2008). In areas with shallow water tables, groundwater is tightly coupled with land surface and energy processes (i.e., a bidirectional relationship with both groundwater recharge and evapotranspiration fluxes), yet this coupling dissipates with deeper water tables and becomes recharge-dominated (i.e., a unidirectional relationship). We use the water table ratio, a derived indicator classifying groundwater-climate interactions as bidirectional or unidirectional (Haitjema and Mitchell-Bruker 2005), to represent groundwater's hydroclimatic function (Cuthbert et al. 2019). Secondly, as the largest store of unfrozen freshwater globally, groundwater provides important storage functions (Gleeson et al. 2020). Net groundwater storage loss is a secondary contributor to global sea level rise (Konikow 2011) while groundwater's large storage capacity also provides important retention and attenuation functions in the water cycle, with system response times that vary from a few to more than 10,000 years. Thus, groundwater naturally serves as an important control on hydrological processes such as floods (Gleeson et al. 2022) and droughts (Van Lanen et al. 2013). As groundwater storage, particularly within depths that are dynamically connected to the Earth system, is challenging to quantify (Gleeson et al. 2016; Ferguson et al. 2021; Condon et al. 2020), we use shallow subsurface porosity (representative for depths on the order of 100m) as a proxy representation of groundwater storage capacity (Gleeson et al. 2014).

To represent *ecosystem* functions, we consider the type and density of groundwater-dependent ecosystems (GDEs). GDEs are terrestrial, aquatic, or subterranean ecosystems that rely on groundwater, occurring either in the subsurface or as surface discharge, for some or all of their freshwater needs (Kløve et al. 2011). We focus on terrestrial and aquatic GDEs as these ecosystem types are more closely coupled to land-surface processes, are better understood in contrast to subterranean ecosystems, dominate conservation and management dialogues (Saito et al. 2021; Rohde et al. 2017), and have been mapped via an inference-based method globally (Huggins et al. 2023). Terrestrial GDEs exist where root systems source groundwater and thus rely on the subsurface presence of groundwater. Conversely, aquatic GDEs rely on surface expressions of groundwater, and include rivers, streams, and wetlands.

Groundwater provides many important economic functions, such as for uses in mining, manufacturing, energy generation, and agriculture which is the dominant form of socioeconomic interaction between humans and groundwater systems at the global scale (Wada et al. 2012; Giordano and Villholth 2007). On this basis, we selectively focus on the *food system* interactions with groundwater. The food system dimensions we include are the extent of areas irrigated with groundwater and farm field size. Including areas irrigated with groundwater enables the archetypes to reflect areas where agricultural actors have the infrastructure to source groundwater for irrigation needs and differentiate regions based on agricultural reliance on groundwater. Secondly, though not often incorporated in groundwater studies, field size is a key attribute of agricultural systems that is associated with many functional differences in groundwater interactions, impacting livelihoods, agricultural practices, and productivity (Meyfroidt 2017). For instance, small scale farms, especially in developing countries, are more likely to have less access to basic services and infrastructure (Meyfroidt et al. 2022) yet contribute significantly to local crop production and nutritional diversity (Ricciardi et al. 2018; Herrero et al. 2017). Conversely, large irrigated farms are generally associated with higher productivity and levels of economic development through mechanisation (Meyfroid 2017). Thus, including field size (which is related to farm size) (Graesser and Ramankutty 2017; Lesiv et al. 2019), enables a contextualisation of the scale and function of food system interactions with groundwater in the archetypes.

Our inclusion of water management systems is an effort to represent what social actors “do within governance [frameworks] related to the development and protection of groundwater” (Villholth and Conti 2018). Thus, our conceptualisation of water management systems aims to represent societal forms of interaction with groundwater resources expressed through policy measures, collective action, and priority setting. Inversely, societal interactions with groundwater systems form values and worldviews that in turn can shape water management practices. We first consider water management systems through the lens of integrated water resources management (IWRM). We use indicators from a global IWRM tracking initiative (UNEP 2021) that explicitly relate to groundwater and represent the level of dedicated management efforts. These include reporting on the measures of “basin/aquifer management plans”, “basin/aquifer level organisations”, and “aquifer management instruments”. Secondly, to consider the role of water management regarding groundwater access, equity, and the domestic services of groundwater, we integrate fundamental data on the percentage of people that collect or use unimproved drinking water. This unimproved drinking water can come from many sources, including an unprotected dug well or spring, or alternatively from surface water sources such as a river, pond, or canal, but these sources are unable to be isolated within the provided indicator. Yet, we view this indicator as a useful and best available representation of groundwater’s utilisation, or lack thereof, in supporting domestic functions and water security.

This global, data-driven approach requires a reductionist view of groundwater functions where the focus is placed on dominant, large-scale processes. While this bias towards dominant processes is commensurate with the guideline for archetypes to operate at an intermediate level of system abstraction (Oberlack et al. 2019), we acknowledge this approach omits many local-scale functions such as cultural values and ecosystem services deriving from groundwater.

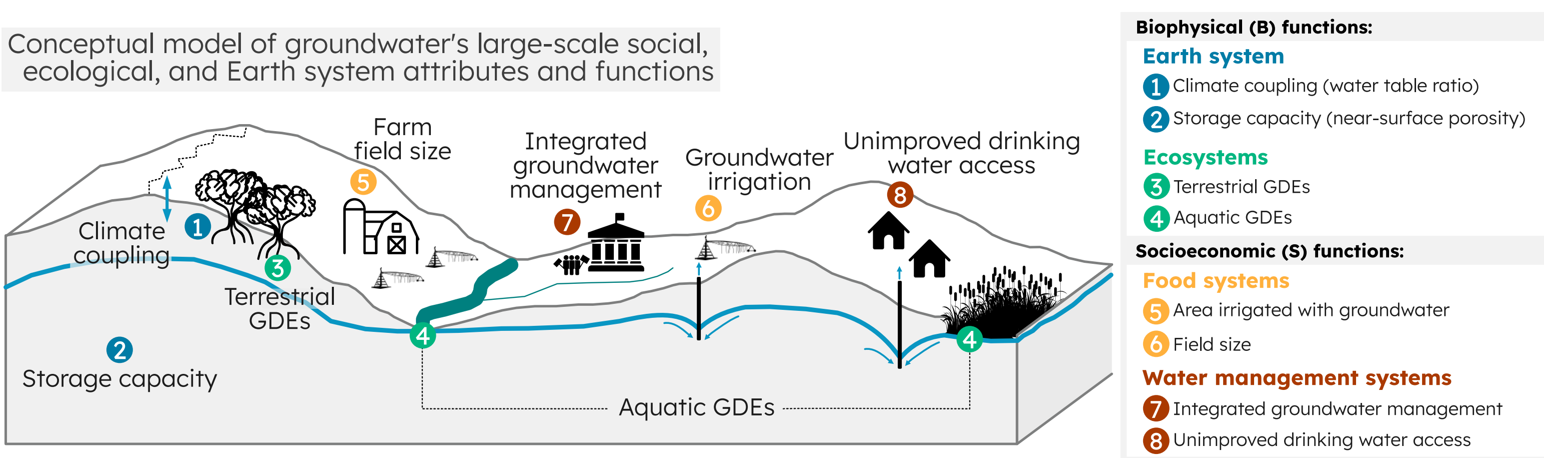

Figure 1. Conceptual model of groundwater’s large-scale socioeconomic, ecological, and Earth system functions that together form the basis of the derived groundwater archetypes.

2.2 Spatial resolution and data pre-processing

We conducted our archetyping analysis at the spatial unit of individual grid cells at 5 arcminute resolution (~10 km at the equator). We selected 5 arcminute grid cells as it balances the base resolutions of the input datasets (Table 1), and produces a moderate-level resolution global data product that is compatible with a wide array of global hydrological models and studies. Secondly, while watersheds are increasingly used to delimit social-ecological system boundaries (e.g., Varis et al. 2019), our approach of applying a moderate-resolution grid enables the identification of sub-watershed variation of archetypes and is common in the archetyping literature (e.g., Sietz et al. 2011; Beckmann et al. 2022).

Input datasets were preprocessed (Figure 2a) to generate a spatially harmonised set of input data. Subsequently, we normalised all data sets such that grid cell distributions held the properties of zero mean and unit variance. Only grid cells for the global land area were included, as defined by the Global Self-consistent, Hierarchical, High-resolution Geography (GSHHG) Database's Global Earth Mask (Wessel and Smith 1996) as provided through the Generic Mapping Tools (GMT) platform (Wessel et al. 2019). Two exceptions were applied to the water management systems datasets, which are derived at the nation and watershed scales. Thus, for these two datasets, the normalisation procedures were performed on the nation-scale and watershed-scale data, respectively, before conversion to raster format. These normalisation procedures ensured that each input dataset would contribute equally to the archetyping outcomes. Data sources, descriptions, and summaries of preprocessing steps applied to each dataset are provided in Table 1.

Before performing the archetyping procedure, we evaluated the collinearity of the eight normalised input datasets (Figure S1). There are moderate levels of collinearity ($r^2 \approx 0.5$) between certain inputs, such as between aquatic and terrestrial GDE density, but no correlation values were sufficiently high to require further modification when using common thresholds to evaluate detrimental levels of collinearity ($r^2 > 0.7$) (Dormann et al. 2013).

Table 1: Input datasets used for archetype derivation. Maps of each input dataset are shown in Figure S2.

Dataset	Data source, information, and preprocessing
Water table ratio	**Data source**: Cuthbert et al. (2019) **Persistent web-link**: https://doi.org/10.6084/m9.figshare.7393304.v8 **Spatial resolution**: 1 km **Temporal range**: Ca. 2000

	Harmonisation: Bilinear resampling to 5 arcminute grid. **Additional preprocessing:** Regions with recharge <5 mm/yr were set to the minimum normalised input value to represent unidirectional (i.e., recharge dominated conditions). We do this following Cuthbert et al. (2019) who masked-out these regions given the variable is highly sensitive to low recharge rates and as these arid regions typically have deep water tables with minimal evapotranspiration fluxes from groundwater. We used the same recharge dataset (Döll and Fiedler 2008) as used in Cuthbert et al. (2019) to apply this mask.
Porosity	**Data source**: Gleeson et al. (2014) **Persistent web-link**: https://doi.org/10.5683/SP2/DLGXYO **Spatial resolution**: Polygons with average size of ~14,000 km^2 **Temporal range**: N/A **Harmonisation:** Vector polygon rasterization to 5-arcminute grid.
Groundwater-dependent ecosystem types (both aquatic and terrestrial)	**Data source**: Huggins et al. (2023) **Persistent web-link**: https://doi.org/10.5683/SP3/P3OU3A **Spatial resolution**: 30 arcsecond **Temporal range**: ca. 2015 **Harmonisation:** Area density calculated per 5-arcminute grid.
Area irrigated with groundwater	**Data source**: Siebert et al. (2010) **Persistent web-link**: https://www.fao.org/aquastat/en/geospatial-information/global-maps-irrigated-areas/latest-version/ **Spatial resolution**: 5-arcminute **Temporal range**: 2000 **Harmonisation:** None
Farm field size	**Data source**: Lesiv et al. (2019) **Persistent web-link**: https://pure.iiasa.ac.at/id/eprint/15526/ **Spatial resolution**: ~1 km **Temporal range**: ca. 2010-2016 **Harmonisation:** Modal resampling to 5-arcminute grid.
Integrated groundwater management	**Data source**: IWRM Data Portal (UNEP 2021) **Persistent web-link**: http://iwrmdataportal.unepdhi.org/ **Spatial resolution**: Nation scale **Temporal range**: 2020 **Harmonisation:** Vector polygon rasterization to 5 arcminute grid **Additional preprocessing:** Countries without data (n = 12) are assigned data of their most-similar country with available water management data. We base country-to-country similarity on the Worldwide Governance Indicators database (Kaufmann et al. 2011; World Bank 2023), using Euclidean distance between country values reported for the year 2020. Countries missing data include Argentina, Brunei, Canada, Djibouti, Eritrea, Uruguay, Venezuela, and several small island nations.
Unimproved drinking Water	**Data source**: World Resources Institute's Aqueduct Water Risk Atlas (Kuzma et al. 2023) **Persistent web-link**: https://www.wri.org/data/aqueduct-global-maps-40-data **Spatial resolution**: HydroBASIN Level 6 **Temporal range**: 2015 **Harmonisation:** Vector polygon rasterization to 5-arcminute grid.

2.3 Two-stage self-organising map to derive archetypes

Social-ecological system archetyping has no consensus methodology (Sietz et al. 2019) and alternative approaches are based on different assumptions and accomplish different objectives. For instance, bottom-up forms of archetyping build from individual case studies and group cases together based on similarity in system composition or behaviour. These bottom-up approaches (e.g., Neudert et al. 2019) are contextually rich yet can be geographically or contextually limited based on the spatial extent, count, and diversity of case studies. Conversely, top-down approaches can use spatially distributed data and derive recurring patterns in empirical data through various methods, including clustering algorithms. Top-down approaches (e.g., Pacheco-Romero et al. 2022) can be limited by the quality and fidelity of data used to represent system attributes, and bias in data selection but can provide a wider and more consistent spatial coverage. Thus, top-down approaches are viewed as more conducive to regional-to-global scales of assessment. The two methodologies may support each other in mixed-method processes (Sietz and Neudert 2022), where bottom-up approaches can aid in ground-truthing archetypes derived from top-down methods (Eisenack et al. 2021).

Quantitative data-driven archetyping can be interpreted as a clustering analysis of data emerging from a specific social-ecological system problem formulation. We summarised these problem formation (Figure 1) and data selection (Table 1) procedures above, and now overview our approach to clustering. There exist myriad algorithmic alternatives to perform clustering, such as partitioning, hierarchical, relational, and density-based approaches (Wierzchoń and Kłopotek 2018). Whereas some studies take the approach of applying a suite of clustering algorithms and select the best performing alternative (e.g., Rocha et al. 2020), there are unavoidable subjective decisions involved in many conventional clustering algorithms, including parameter setting, selecting the number of clusters, and setting cluster membership thresholds (Seitz et al. 2019) which can yield archetype outputs that are be sensitive to these decisions. In this study, we opt to use self-organising maps (SOMs) to derive clusters.

SOMs, which are a form of unsupervised artificial neural network (Kohonen 2001), are increasingly used in archetyping analysis (e.g., Václavík et al. 2013; van der Zanden et al. 2016; Beckmann et al. 2022). SOMs require fewer parameters to be set prior to clustering and are not predicated on distributional assumptions of the underlying input data. Thus, SOMs are perceived as less prone to researcher bias in the clustering process of archetyping (Seitz et al. 2019). SOMs are composed of a lattice of nodes, each possessing a ‘codebook vector’ representing the node's position in the multidimensional data space as defined by the input data. SOM training involves iteratively presenting the input data to the lattice of nodes which learn the distribution of the data. SOMs, among other clustering approaches, uniquely preserve the topology of the input data, meaning that input features assigned to nearby SOM nodes (i.e., clusters) are more similar than features assigned to distant nodes in the lattice. In this way, SOMs are well-suited for exploratory archetyping in comparison to other clustering methods (Seitz et al. 2019).

To derive our groundwater system archetypes, we applied a sequenced, two-stage SOM methodology (Figure 2). The first stage involved training a two-dimensional SOM lattice on the normalised input data (Figure 2b, 2c). The goal of this step was to reduce the volume of data by providing a synthetic representation of the input data space that reflects its topology yet with a considerably smaller set of data points while simultaneously generating an intermediary classification layer that provides greater traceability in the classification procedure between input data points and final archetypes. We refer to the codebook vectors generated by the first SOM as *prototypes*. The second SOM was then trained on the prototypes emerging from the first-stage SOM. The codebook vectors developed through the second-stage SOM represent the function configurations we present as *archetypes* in our study (Figure 2d, 2e). The second SOM was generated using a one-dimensional lattice to enable prime numbers of clusters (and thus archetypes) to be developed and evaluated (e.g., a two-dimensional SOM can not generate a solution for 5 clusters). While it is common to use other clustering algorithms to cluster codebook vectors produced through a SOM (Vesanto and Alhoniemi 2000), we followed Delgado et al. (2017) by using a second SOM to classify the first SOM's codebook vectors, which presents the first application of this specific sequenced SOM methodology to the archetyping literature. More granular details, including how the ranges of SOM sizes evaluated were determined, performance metrics, and reproducibility steps are provided in *Section 2.4 Full workflow details*.

2.4 Full workflow details

We based our clustering approach on the two-stage SOM clustering workflow developed by Delgado et al. (2017) and made modifications to follow archetyping best practices (Eisenack et al. 2019) and to navigate function availability in open-source software. Following Delgado et al. (2017), we did not set specific SOM lattice sizes *a priori* for either stage but instead iterated through a range of possible SOM sizes in each stage and selected the best-performing SOM based on an integrated performance metric.

For the first-stage SOM (Figure 2b), we iterated across SOM lattice sizes ranging from 10x10 to 30x30, increasing at increments of 2x2 (i.e., 10x10, 12x12, 14x14, …, 30x30). This range was determined based on the underlying heterogeneity in the input data and the derivation of this range is shown in the Supporting Information (Text S1). As SOMs are sensitive to initialisations of the node codebook vectors, we reproduced multiple (20) SOMs for each lattice size as suggested by Delgado et al. (2017). We calculated SOM performances using an integrated metric, further described below, that considers both topographic error and explained variance and selected the SOM iteration that minimised this metric (Figure 2c). Topographic error is a SOM-specific quality metric which represents how well the topography of the input data is preserved in the SOM, and is calculated as the proportion of all input data points whose assigned (i.e. closest) SOM node and second-closest SOM node (closeness determined in Euclidean space) are not adjacent nodes in the SOM lattice (Kohonen 2001).

To select the best-performing SOM in this first-stage, we first screened for performance outliers at each SOM and selected the remaining SOM iteration with the best integrated performance metric score. We screened for outliers at each lattice size to additionally minimise the non-deterministic nature of SOMs. As we observed a range of performance scores for each SOM lattice size, we sought to develop a methodology that would select a SOM size that is both reflective of overall performance trends across different SOM sizes while still selecting a SOM iteration that performs well relative to the competing iterations generated at the same SOM size. That is, we found that the best-performing SOM size would vary between repetitions of the iterative approach whereas the best-performing size was stable (routinely reproduced) when outliers were removed. Thus, we opted to prioritise reproducibility over absolute SOM performance by applying this performance outlier screening. We screened for outliers by setting narrow outlier thresholds of the median ± the median absolute deviation in the integrated performance metric.

For each first-stage SOM size, the integrated performance metric (Text S2) combined topographic error and unexplained variance (i.e., 1 - explained variance). We combined both metrics into an integrated metric by variance-normalising, summing, and finally min-max scaling. Applying variance-normalisation ensured that each metric contributed equally to the integrated performance score as otherwise a metric with greater internal variation would impart a greater effect on the integrated metric. We sought to avoid this as metric-specific variation ranges are a product of each error metric's formulation and thus are challenging to compare and integrate at face-value. We min-max scale the integrated performance score simply to ease the interpretation of the metric (with a value of 0 as best and 1 as worst). This procedure enables the identification of the SOM size which best balances trade-offs between minimising topographic error and maximising the percentage of variance explained in the input data.

For the second-stage SOM (Figure 2d), we developed SOMs across the range of lattice sizes from 1x4 to 1x30, increasing in 0x1 increments (i.e., 1x4, 1x5, 1x6, …, 1x30). This range is set based on the recommended range of archetypes to identify in a given archetyping study (Eisenack et al. 2019). This second-stage SOM classified the prototypes derived from the first-stage SOM into the final set of archetypes. Just as was done for the first-stage SOM, we reproduced multiple (100) SOMs for each lattice size and selected the best-performing SOM iterations based on a similarly developed integrated performance metric (Figure 2e). As the number of prototypes is substantially fewer than the size of the input dataset, we were able to generate a greater number of alternative SOMs at each lattice size.

We evaluated the second-stage SOMs using the same error metrics as the first-stage SOM (i.e., topographic error and unexplained variance) and added an additional penalty metric based on the number of nodes in the SOM. The motivation for this stems from an underlying motivation of archetyping: to develop intermediate levels of system classification with the ambition of bridging "global narratives with local realities" (Oberlack et al. 2019). Thus, archetyping analysis is characteristically different from standard clustering as it seeks to not only identify meaningful groups of data points but to additionally develop narratives for these derived groups. Given that it is more conducive to develop narratives with a smaller number of archetypes, and that scale is intuitively perceived logarithmically (Varshney and Sun 2013), we included a quantitative performance metric that would bias towards a smaller number of archetypes. Thus, we added a penalty term in our performance metric for these second-stage SOMs that was calculated as the logarithm of the number of derived clusters (Text S2). All other steps were performed identically to the first-stage SOM, including variance-normalising each performance metric, summing across metrics, and min-max scaling of the integrated performance metric, the screening for performance outliers at each lattice size, and the selection of the best-performing SOM from the remaining iterations.

Together, the sequenced, two-stage SOM procedure generated a crisp clustering of the data with a nested membership structure where each of the ~2 million grid cells is a member of one prototype, and each prototype is a member of one archetype (Figure 2f). Though this membership structure, prototype and archetype results are mapped back to geographic space.

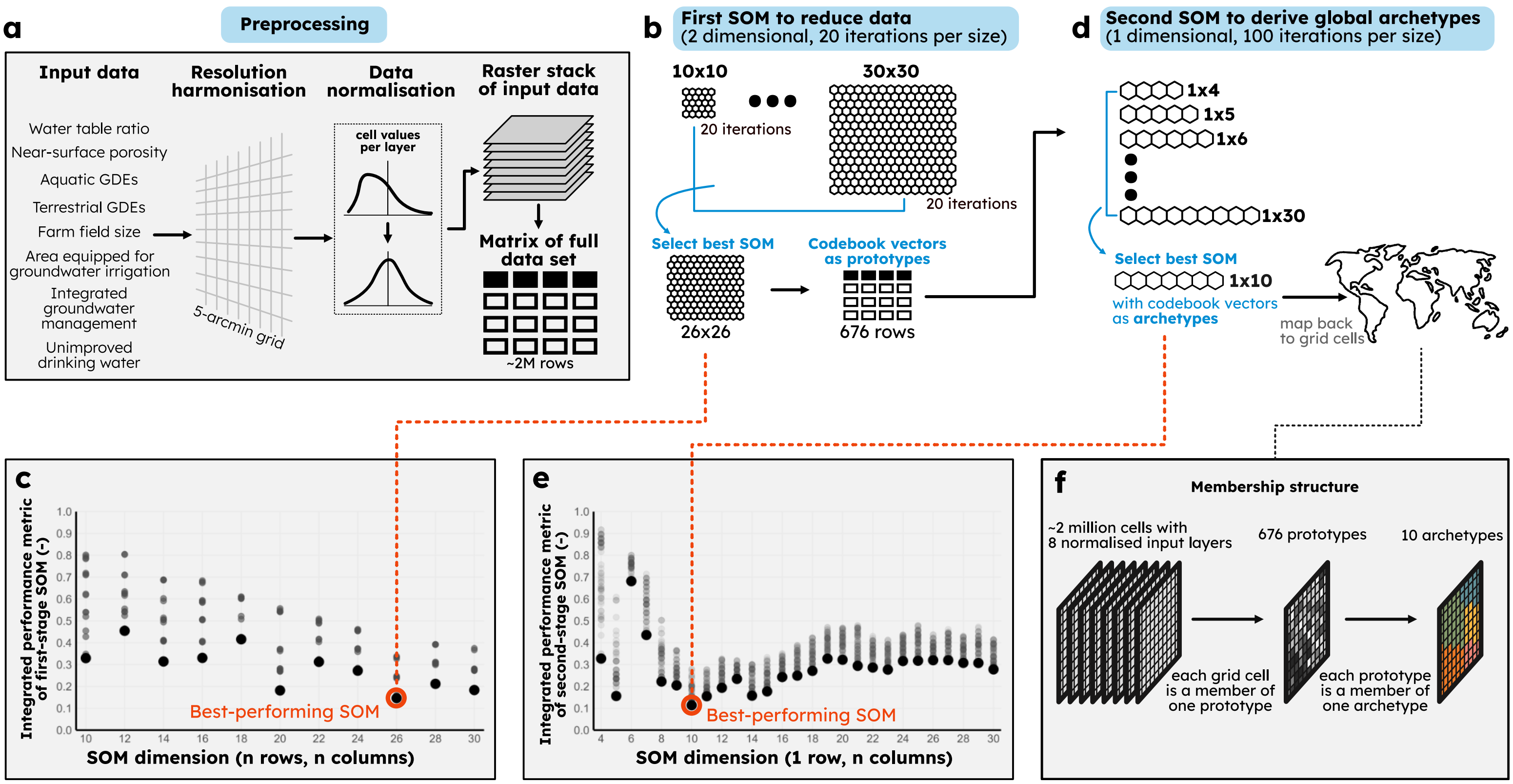

Figure 2. Archetype derivation process. (a) Data preprocessing. (b) The first-stage SOM iterations, with the goal of simplifying the input data space into a representative set of prototypes. (c) The integrated performance metric identified a 26x26 SOM as the best-performing SOM iteration, whose codebook vectors are used as the derived prototypes. (d) The second-stage SOM iterations, which are trained on the prototypes emerging from the first-stage SOM. (e) The integrated performance metric identified a 1x10 SOM as the best-performing SOM iteration, whose codebook vectors are used as the derived archetypes. (f) This approach provides a crip archetyping classification, meaning each grid cell is a member of one prototype and each prototype is a member of one archetype.

The full input data size was computationally prohibitive to implement on the deeply iterative first-stage SOM (~2 million data points with 8 attributes and 20 SOM iterations for each of 11 alternative SOM sizes). To reduce this burden, we took a sample of the full data that satisfied a threshold of representing 95% of the underlying patterns in the data (described in Text S3). We consistently found that a sample size of n = 350,000 met this threshold and reduced the data volume by a factor of ~6. Thus, the first-stage SOM was trained on a sample of 350,000 data points rather than on the full set of ~2 million points. For all data points (grid cells) not included in the sample, prototypes were assigned based on each data point's nearest neighbour (using Euclidean distance) in the input feature space that was included in the sample set. To test the impact of this sampling procedure and the robustness of the archetypes, we repeated our clustering approach on five alternate sample sets of the same size that fit the same coverage criterion described above. We describe the results of this robustness analysis in Section 3.5, and full details of our approach can be found in Text S4.

We calculated several landscape metrics to evaluate the spatial distribution of archetypes. Globally, we assessed class adjacency rates, which represent how many grid cell edges are shared between archetypes and provide information about the frequency of archetypes being situated next to one another. Within the 37 large aquifer systems of the world (Margat 2008), we computed the area distribution of archetypes, as well as the Simpson's evenness index (Simpson 1949), the contagion index (Riitters et al. 1996), marginal entropy and relative mutual information (Nowosad and Stepinski 2019). Simpson's evenness index is a diversity metric that represents if archetypes are evenly distributed relative to the number of archetypes found within the aquifer (index is high) or if there is dominance of some archetypes (index is low). The contagion index is an aggregation metric that represents the likelihood that two adjacent grid cells belong to the same archetype. Marginal entropy measures the thematic complexity of archetypes within an aquifer, while relative mutual information has been shown to be a useful approach to differentiate landscape patterns that otherwise show similar levels of thematic complexity (Nowosad and Stepinski 2019). Calculating these landscape metrics for archetype distributions within the large aquifer systems of the world facilitates the exploration of spatial patterns of archetypes within these aquifer systems and enables grouping of these aquifers based on the similarity of their archetype distributions.

3 Results and discussion

3.1 Unique patterns in groundwater functions reveal the need for archetyping

To address the question "is this archetyping necessary?", we begin by exploring the underlying heterogeneity of groundwater's socioeconomic, ecological, and Earth system functions in the absence of archetyping. To do so, we mapped the Earth system, ecosystem, food system, and water management system functions identified in our conceptual model using baseline classification schemes for each input dataset (Figure 3), which is instructive for two independent reasons. Firstly, this mapping reveals spatial patterns in groundwater functions (Figure 3a-d) that had yet to be synthesised, and which are described in the following paragraphs. Secondly, this exercise revealed over 79,000 unique system configurations when overlaying all functions simultaneously (Figure 3e). Archetyping thus becomes a necessary endeavour to extract and summarise common and representative patterns in these deeply heterogeneous systems (Sietz et al. 2019) that otherwise would present an overwhelming and intractable diversity of system types to interpret (Oberlack et al. 2019).

To explore patterns in groundwater's biophysical functions, we individually mapped groundwater's Earth system (Figure 1a) and ecosystem functions (Figure 1b). For the mapped Earth system functions (Figure 3a), we observe three leading patterns: areas where storage capacity is high and climate coupling is unidirectional (such as in the Sahara), areas where storage capacity is low and climate coupling is bidirectional (such as in the local and shallow aquifers with low productivity across Western Africa), and areas where storage capacity is high and climate coupling is bidirectional (such as across the western Amazon and the Okavango Basin). Ecologically (Figure 3b), most areas of the world are characterised by low GDE densities. However, high densities of both aquatic and terrestrial GDEs occur in Southeastern Asia, the Amazon, and western Africa. Aquatic GDEs dominate the landscape in regions including the Congo Basin and Eastern China. Conversely, terrestrial GDEs are extensive across the Sahel, central India, northern Australia, and northeastern China.

To explore patterns in groundwater's socioeconomic functions, we individually map groundwater's food system (Figure 1c) and water management system (Figure 1d) functions. Amongst agricultural lands, most areas are characterised by low densities of groundwater irrigation (Figure 3c). Low groundwater irrigation densities in regions predominantly characterised by small field sizes include Sub-Saharan Africa, while those predominantly characterised by large field sizes include the Canadian Prairie, Australia, and the Eurasian wheat belt. Conversely, small farms with extensive groundwater irrigation are found across the Indian Subcontinent and the North China Plain. Large farms with extensive groundwater irrigation are found in the American Midwest, Northern France, and in regions of Argentina and Brazil. Generally, integrated groundwater management and unimproved drinking water access demonstrate an inverse relationship and nations with high levels of groundwater management tend to have low levels of unimproved drinking water access. Yet, nations where we see higher levels of unimproved drinking water access in areas with moderate groundwater management include Morocco and Kenya, while countries with lower levels groundwater management that also have low levels of unimproved drinking water access include Chile, Egypt, and Thailand.

While certain patterns, such as those described above, are discernible for individual maps in Figure 3, manually analysing patterns across all functions is intractable. Thus, we turn to archetyping analysis to extract and quantify these patterns.

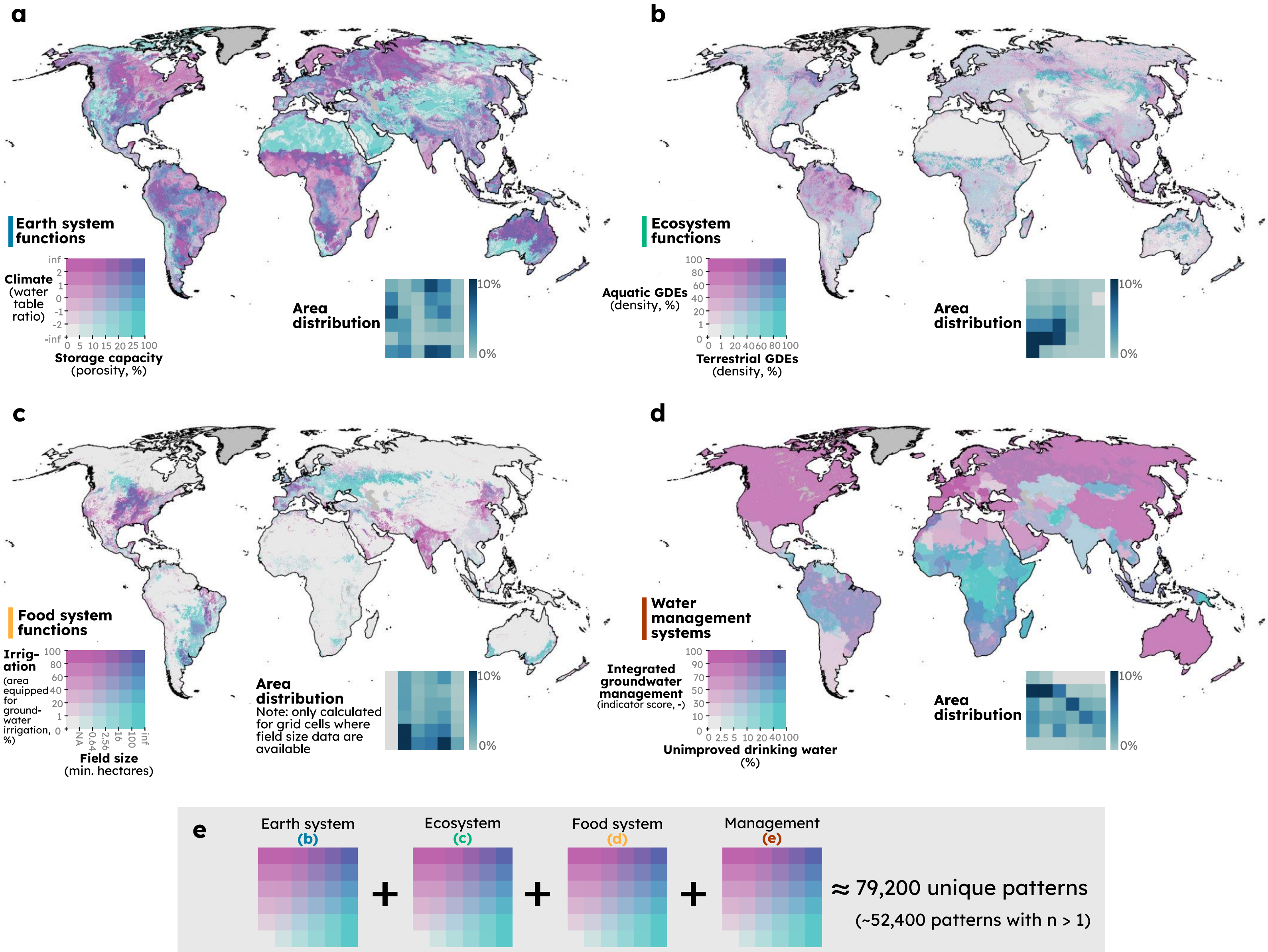

Figure 3. Exploratory mapping of groundwater interactions with (a) Earth systems, (b) ecosystems, (c) food systems, and (d) water management systems. (e) Overlaying these four bivariate maps revealed over 79,000 unique patterns, highlighting the potential and need for

archetyping. The area distribution of each mapped bivariate relationship is shown by inset heatmaps accompanying each map, and which have the same axis breaks as shown in each map's legend. For the area heatmap for food system functions, we show the area distribution only for areas where grid cell data exists for both groundwater irrigation and field size.

3.2 Ten groundwater archetypes

Our archetyping analysis generated a set of 10 groundwater archetypes (Figure 4a). These groundwater archetypes (GAs) provide a first assessment of the dominant spatial patterns in groundwater's socioeconomic, ecological, and Earth system functions. The archetypes were derived from a first-stage SOM, with a lattice size of 26x26, that generated a set of 676 prototypes (Figure 2c), and a second-stage SOM, with a lattice size of 1x10, that generated the set of 10 archetypes (Figure 2e). Individual archetypes are described in Table 2 and extents of individual archetypes are shown in Figure 4c.

Each archetype presents a unique and representative configuration of groundwater's socioeconomic, ecological, and Earth system functions that reoccur over broad spatial extents (Figure 4b). GA2 is the most extensive archetype, covering 17.5% of the terrestrial surface area included in our analysis, while GA5 has the smallest extent and covers 4.9% of the analysed area. Thus, the archetypes contrast the overlaying of individual groundwater functions (shown in Figure 3) which also provide unique configurations ($n \approx 79{,}200$) but apply to only very small areas (median extent of 0.00014%) and thus are not broadly applicable (Figure S3). Plotting the distribution of individual functions within archetypes (Figure 5) reveals these broadly occurring configurations, such as GA5 which is uniquely characterised by smallholder farms highly reliant on groundwater for irrigation or GA8 which is uniquely characterised by high aquatic and terrestrial GDE density and large groundwater storage capacity. Plotting these function ranges within archetypes also reveal similarities between archetypes, such as GA6 and GA7 both being characterised by largeholder farms, and GA4 and GA10 both being characterised by limited groundwater management and elevated rates of unimproved drinking water access.

We observe broad spatial patterns in the archetypes, such as extensive areas of GA1 (*Minimal Earth system, ecosystem, and food system functions*) and GA2 (*Large storage capacity but minimal other functions*) throughout arid and high-latitude remote regions, including the Sahara, northwestern China, and eastern Siberia. GA8 (*Extensive GDEs with elevated Earth system functions but limited food system functions*) is found extensively throughout the Amazon, while archetype GA6 (*Largeholder farming with some groundwater dependence and moderate Earth* *functions*) is found throughout the American Midwest. Conversely, GA7 (*Largeholder farming with some groundwater irrigation and extensive aquatic GDEs*) is found across southern Brazil and Uruguay. There are also areas that have interspersed archetype distributions, including in northeastern China, the southern Iberian peninsula, and eastern Brazil, which correspond to regions with greater local variation in the groundwater functions included in our analysis.

We performed grid cell adjacency analysis (Figure 6) to investigate the frequency of archetype pairings in adjacent grid cells. For every archetype, we find that any grid cell of the given archetype is most likely to neighbour with grid cells of the same archetype, confirming that the derived archetypes are generally clustered geographically. Given that geographic location was not included as an input feature for the archetyping analysis, the outcome that most archetype grid cells are spatially clustered indicates that the archetyping approach robustly produced archetypes that reflect broad patterns in groundwater functions. Investigating the highest frequency neighbouring archetype pairs also reveals underlying similarities and natural transitions between archetypes. For instance, 11% of all pairwise edge connections with GA6 are shared with GA7, and both of these archetypes are characterised by largeholder farming with moderate dependence on groundwater for irrigation but whereas GA7 possesses extensive aquatic GDEs, GA6 is characterised by low GDE densities.

Table 2: Descriptions of the ten groundwater archetypes (GA). Characteristic function magnitudes show the function magnitude per archetype relative to the mean function magnitude across all archetypes with upper and lower bounds shown as half of each function's standard deviation. Legend for characteristic function magnitudes: C = climate coupling, S = storage capacity, T = terrestrial GDEs, A = aquatic GDEs, F = field size, I = area irrigated with groundwater, M = integrated groundwater management, D = unimproved drinking water access.

GA #	***Name*** **and Description**	**Characteristic function magnitudes**	**Example regions**
1	*Minimal Earth system, ecosystem, and food system functions* Recharge-dominated climate interactions, low storage capacity, sparse groundwater-dependent ecosystems, little groundwater-dependent agricultural activity, and in jurisdictions with a wide range but generally high levels of integrated groundwater management.	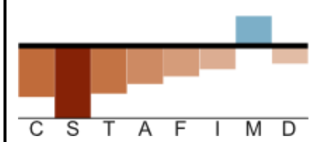	Siberia, uninhabited regions of Arabian Peninsula, The Namib
2	*Large storage capacity but minimal other functions* Recharge-dominated climate interactions, large storage capacity, sparse groundwater-dependent ecosystems, low levels of groundwater irrigation, and in jurisdictions with a wide range of integrated groundwater management.	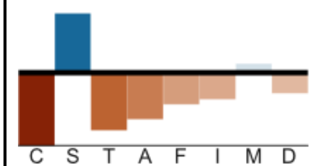	Sahara, Siberia, southern Australia
3	*Earth system functions in jurisdictions with generally high levels of water management* Bi-directional climate interactions (i.e., both recharge and evapotranspiration fluxes), moderate storage capacity, low groundwater-dependent ecosystem densities, little groundwater-dependent agricultural activity, and very high levels of integrated groundwater management.	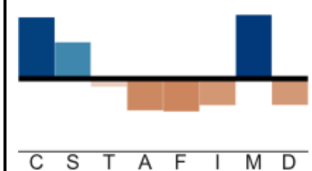	Boreal forests of Canada, northern Australia
4	*Climate functions in regions with limited water management and underserved populations* Bi-directional climate interactions, sparse groundwater-dependent ecosystems, low levels of groundwater-dependent agricultural activity, and high rates of unimproved drinking water access in jurisdictions with very low levels of integrated groundwater management.		Sahel, central Argentina
5	*Smallholder farming highly dependent groundwater* Variable climate interaction modes, moderate storage capacity, low groundwater-dependent, often smallholder farms with very high dependence on groundwater for irrigation, generally low rates of unimproved drinking water access, in jurisdictions with variable levels of integrated groundwater management.	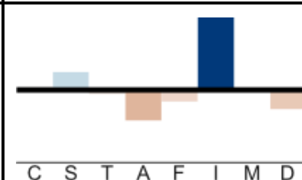	Indian subcontinent, North China Plain
6	*Largeholder farming reliant on groundwater irrigation with moderate Earth functions* Variable climate interaction modes, moderate storage capacity, low groundwater-dependent ecosystem density, largeholder farms with moderate dependence on groundwater irrigation, across jurisdictions with a wide range of groundwater management, and generally low rates of unimproved drinking water access.	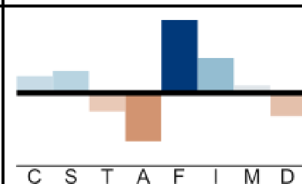	US northern Midwest, Buenos Aires Province (Argentina)

7	*<u>Largeholder farming with some groundwater irrigation and extensive aquatic groundwater-dependent ecosystems</u>* Variable climate interaction modes, High aquatic groundwater-dependent ecosystem densities, very large farms with moderate dependence on groundwater for irrigation, in jurisdictions with a wide range in groundwater management and low rates of unimproved drinking water access.	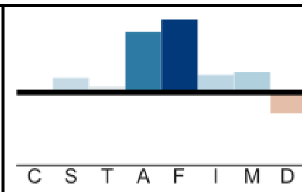	Southern Brazil, western non-mountainous Europe
8	*<u>Extensive groundwater-dependent ecosystems with moderate Earth system functions but limited agricultural functions</u>* Large storage capacity, extensive aquatic and terrestrial groundwater-dependent ecosystems, low levels of groundwater irrigation, and variable rates of both unimproved drinking water access and implemented groundwater management.		Amazon, Indonesia, Bangladesh
9	*<u>Extensive groundwater-dependent ecosystems with small storage capacity and limited agricultural functions</u>* Variable climate interactions modes, small storage capacity, variable climate interactions, high aquatic and terrestrial groundwater- dependent ecosystem densities, low levels of groundwater irrigation, with a wide range in groundwater management and generally low rates of unimproved drinking water access.	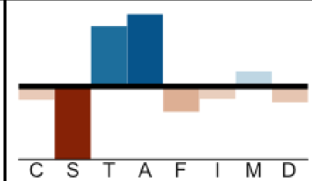	Quebec (Canada), northeastern Brazil
10	*<u>Underserved populations with limited water management systems</u>* Variable climate interactions modes, small storage capacity, moderate aquatic groundwater-ecosystem densities, low levels of groundwater irrigation, in jurisdictions with very little groundwater management and with very high rates of unimproved drinking water access.	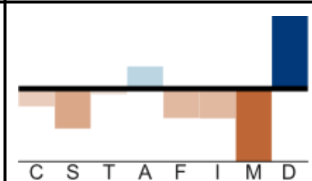	Congo Basin, western Tropical Africa, Afghanistan, Papua New Guinea

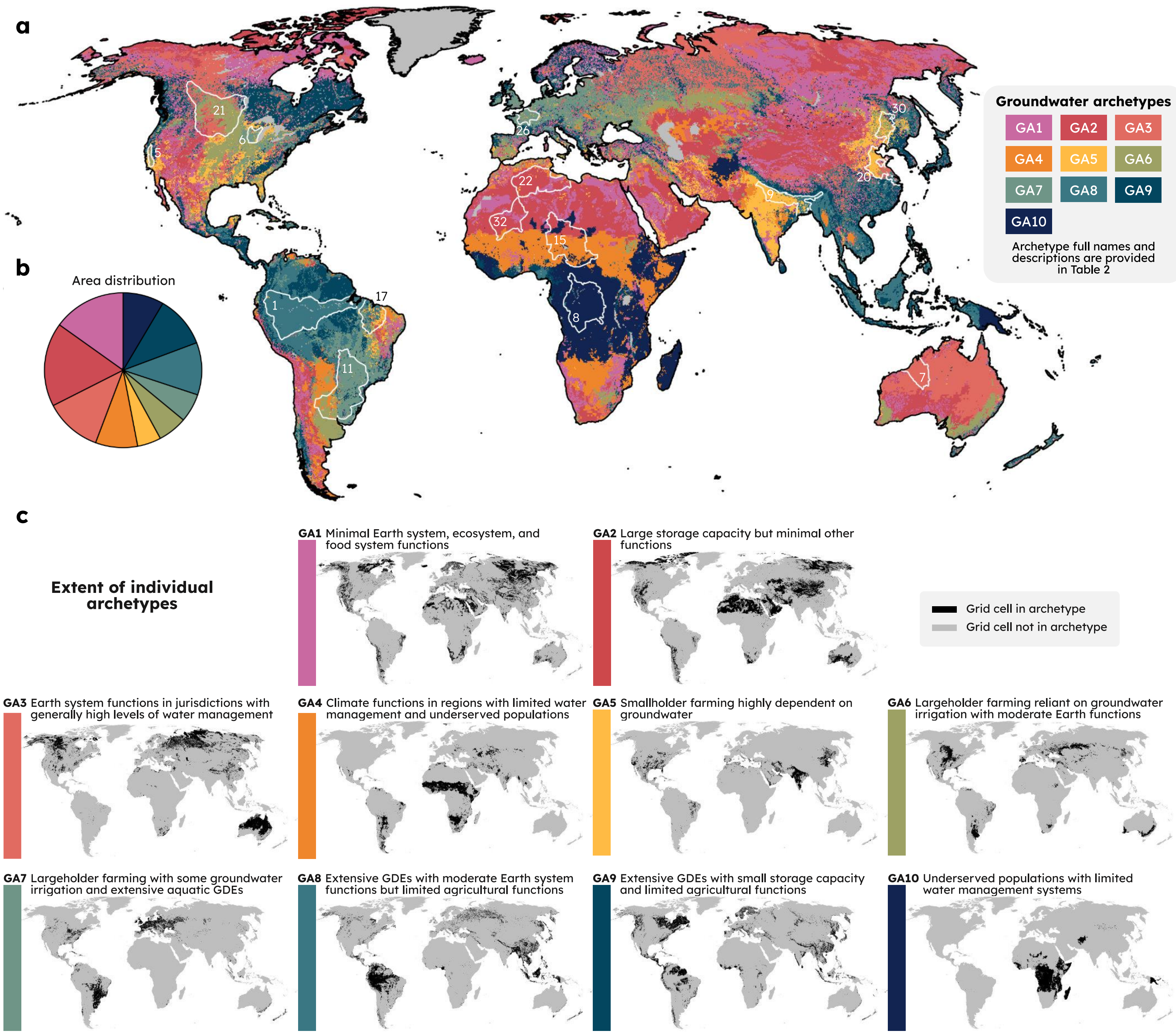

Figure 4: Groundwater system archetypes. (a) Global map of the 10 archetypes. White polygons represent large aquifer systems shown in Figures 6, with the annotated numbers representing aquifer IDs. (b) Area distribution of archetypes. (c) Extent of individual archetypes.

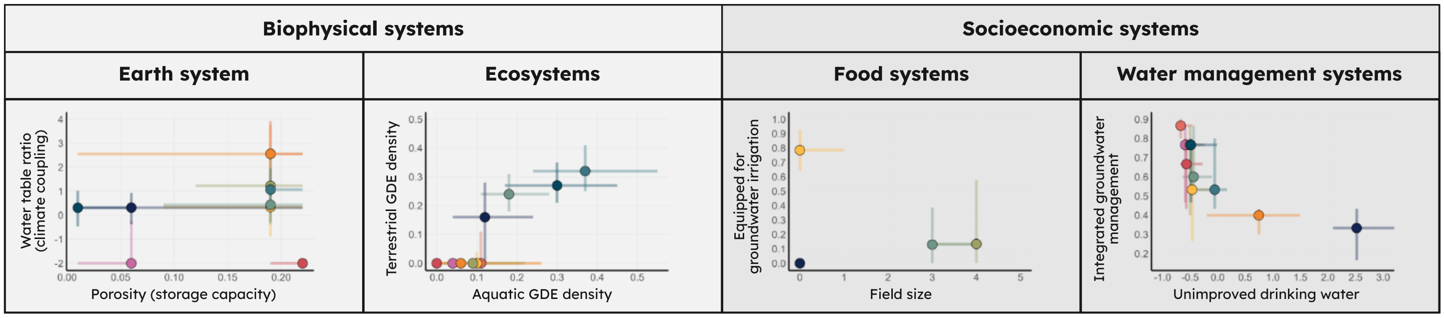

Figure 5: Interquartile function ranges for each archetype. Archetypes are colour-coded to correspond with the legend provided in Figure 4.

Figure 6: Archetype grid cell adjacencies reveal the most common neighbouring archetype pairings. (a) Annotated example for GA1. (b) Grid cell adjacency rates for each individual archetype. (c) Regions exemplifying common archetype pairings identified through grid cell adjacency counts.

3.3 Multiple archetypes in all large aquifers of the world

Every one of the 37 large aquifer systems of the world contain more than one archetype (Figure 6). The Amazon, Canning, and Congo Basins are the least diverse of these large aquifer systems, with only 2 archetypes predominantly found within each system's borders, while the Atlantic and Gulf Coastal Plains (USA), California Central Valley (USA), Karoo Basin (South Africa), Maranhao Basin (Brazil), and the North China Aquifer Systems are the most diverse systems with 8 archetypes predominantly found within each. These heterogeneous archetype distributions across aquifers importantly highlight how, despite being often considered as homogeneous, lumped systems in global groundwater assessments, the processes and groundwater functions that occur within these large aquifer systems are often very heterogeneous.

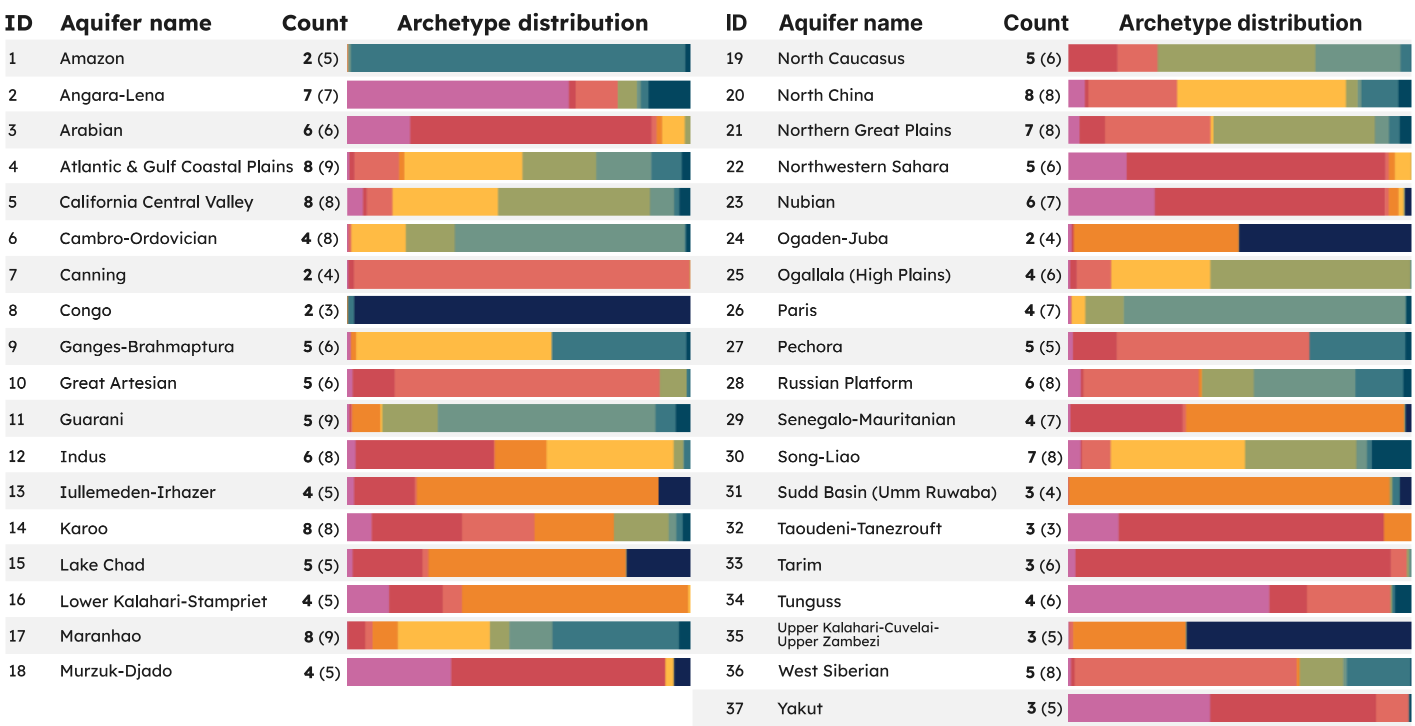

Figure 7: Coverage of archetypes by area within the large aquifer systems of the world. Archetype counts are calculated based on archetypes that cover a minimum threshold of 1% of the aquifer's area (0.1% in parentheses).

Simply counting the number of archetypes within an aquifer provides an introductory but insufficient description of the heterogeneity and distribution of archetypes. For instance, although the Angara-Lena and Song-Liao Basins both contain seven archetypes within their boundaries, it can be observed one archetype (GA1) is relatively dominant and constitutes a considerable combined area proportion of the Angara-Lena Basin, whereas the seven archetypes within the Song-Liao Basin are more equally distributed and are scattered heterogeneously across the aquifer. Thus, we supplemented this analysis by computing several additional landscape metrics to further describe the spatial patterns of archetypes within aquifers (Figure 8).

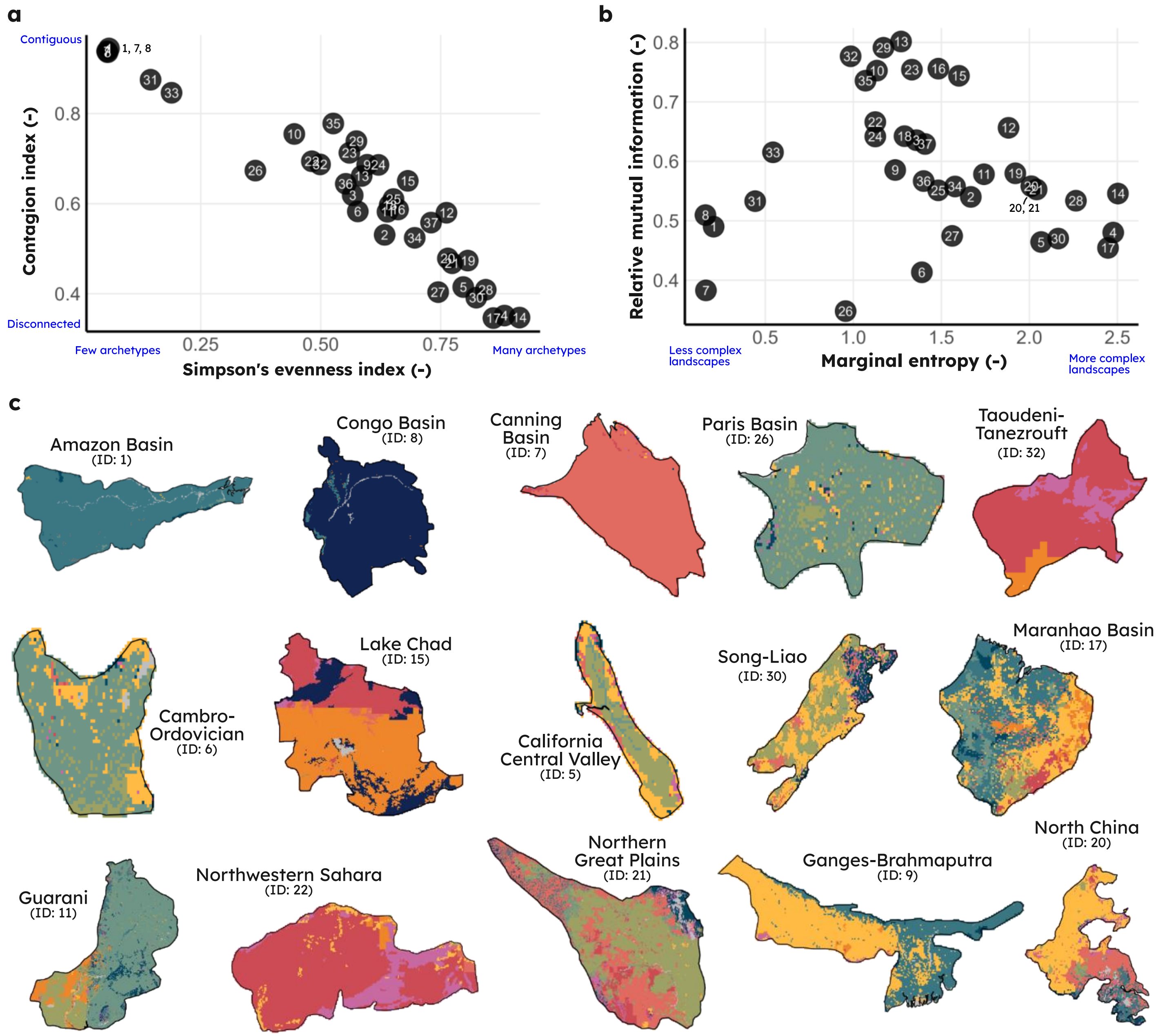

Figure 8: Landscape metrics of archetypes within the 37 large aquifer systems of the world. (a) Plot of Simpson's evenness index (x-axis) and the contagion index (y-axis). (b) Plot of marginal entropy (x-axis) and relative mutual information (y-axis). (c) Archetype distributions within select aquifer systems. Aquifer IDs correspond to the points labels in panels (a) and (b) and also

correspond to the aquifer borders mapped in Figure 4. Inset maps are scaled to optimise visualisation and thus are not shown at a consistent scale.

There is a strong relationship between the Simpson's evenness index and the contagion index of archetypes within aquifers (Figure 8a). These metrics identify aquifers such as the Amazon Basin and the Congo Basin as among the least diverse and most contiguous in their archetype make-up, whereas the Song-Liao Basin (China) and Maranhao Basin are among aquifers with the greatest heterogeneity and diversity of archetypes. Given landscape indices such as the Simpson's evenness index and the contagion index are often correlated, plotting marginal entropy against relative mutual information is one proposed approach to differentiate and classify landscape patterns with weakly uncorrelated indices (Nowosad and Stepinski 2019). When applying this approach (Figure 8b), we are able to differentiate GA patterns between aquifers that contain similar levels of evenness and contiguity. For instance, the Paris and Taoudeni-Tanezrouft Basins show similar levels of evenness and contiguity (Figure 8a) yet the two basins can be differentiated on the basis of relative mutual information, with the Paris Basin demonstrating considerably less relative mutual information (Figure 8b). Such analytical approaches could be useful for applications that would benefit from grouping aquifers based on similarity in their archetype composition.

3.4 Sub-archetype heterogeneity

While archetypes provide a global-level classification of groundwater's socioeconomic, ecological, and Earth system functions, substantial simplifications are necessary to reduce the deeply heterogeneous global landscape into a small set of archetypes. To accomplish this requires the compression of substantial heterogeneity into classes derived based on the most dominant patterns in the underlying data. Doing so results in archetypes with internal heterogeneity, meaning that a range of values is found for each function within each archetype (as shown in Figure 5). Thus, at the individual grid cell, functions will vary from the cell's respective archetype's central value. To explore and quantify the extent of this functional simplification imparted by the archetypes, we investigated the residual between grid cell attributes and their respective archetype (calculated as the Euclidean distance) and mapped the z-score of the residual at the individual grid cell level to facilitate more intuitive interpretation of results (Figure 9).

Regions where grid cell values are far from their respective archetype's central values (large residual) include the American midwest, southern South America, central India, Bangladesh, and Papua New Guinea (Figure 9a). Conversely, regions where grid cells values are quite similar to their archetype's central values include the American southwest, Northern Africa, and Arabian Peninsula, western China, and Siberia. When evaluating these residual distributions per archetype, we can identify GA1 and GA2 as having smaller residual distributions whereas grid cells in GA5, GA6, and GA10 tend to have the largest residual values. One interpretation to explain patterns in these residuals between the archetypes is that archetypes with a small set of clearly distinguishing function combinations (such as GA5 with small field size and very high groundwater irrigation, or GA10 with very low groundwater management and very high rates of unimproved drinking water access) tend to include grid cells that fit these criteria regardless of their other function magnitudes. Conversely, GA1 which is identified uniquely as having minimal functions requires a very specific (narrow) configuration of all input datasets for a grid cell to be classified within the archetype.

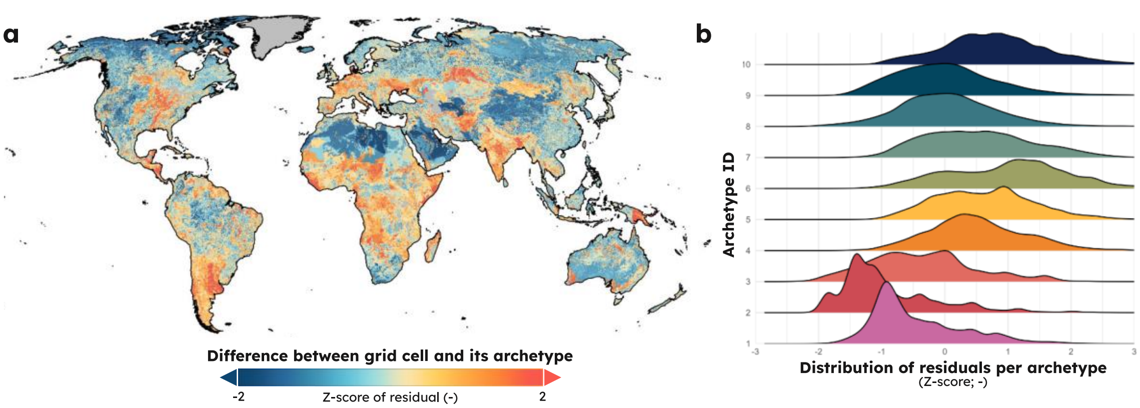

Figure 9: Plotting the functional simplification (information loss) in archetyping at the individual grid cell and archetype level. (a) Z-score of residuals between each grid cell's function attributes and the grid cell's respective archetype's central values. (b) Distribution of grid cell residual z-scores per archetype.

Our sequenced archetyping approach enables further investigation into sub-archetype heterogeneity through the exploration of prototype distributions within archetypes. All archetypes consist of a set of prototypes, ranging from 43-94 prototypes sharing membership with a single archetype (Figure S4). Like archetypes, each prototype is characterised by a unique configuration of groundwater functions and while each prototype is unique, prototypes that are members of the same archetype are more similar than prototypes that are members of different archetypes. To highlight how the prototypes can be used to reveal spatial patterns in sub-archetype heterogeneity, we mapped prototype ranges for two regions where archetypes

596 are spatially extensive and contiguous: GA5 across the Indian subcontinent, and GA10 across
597 the Congo Basin and surrounding regions (Figure 10).

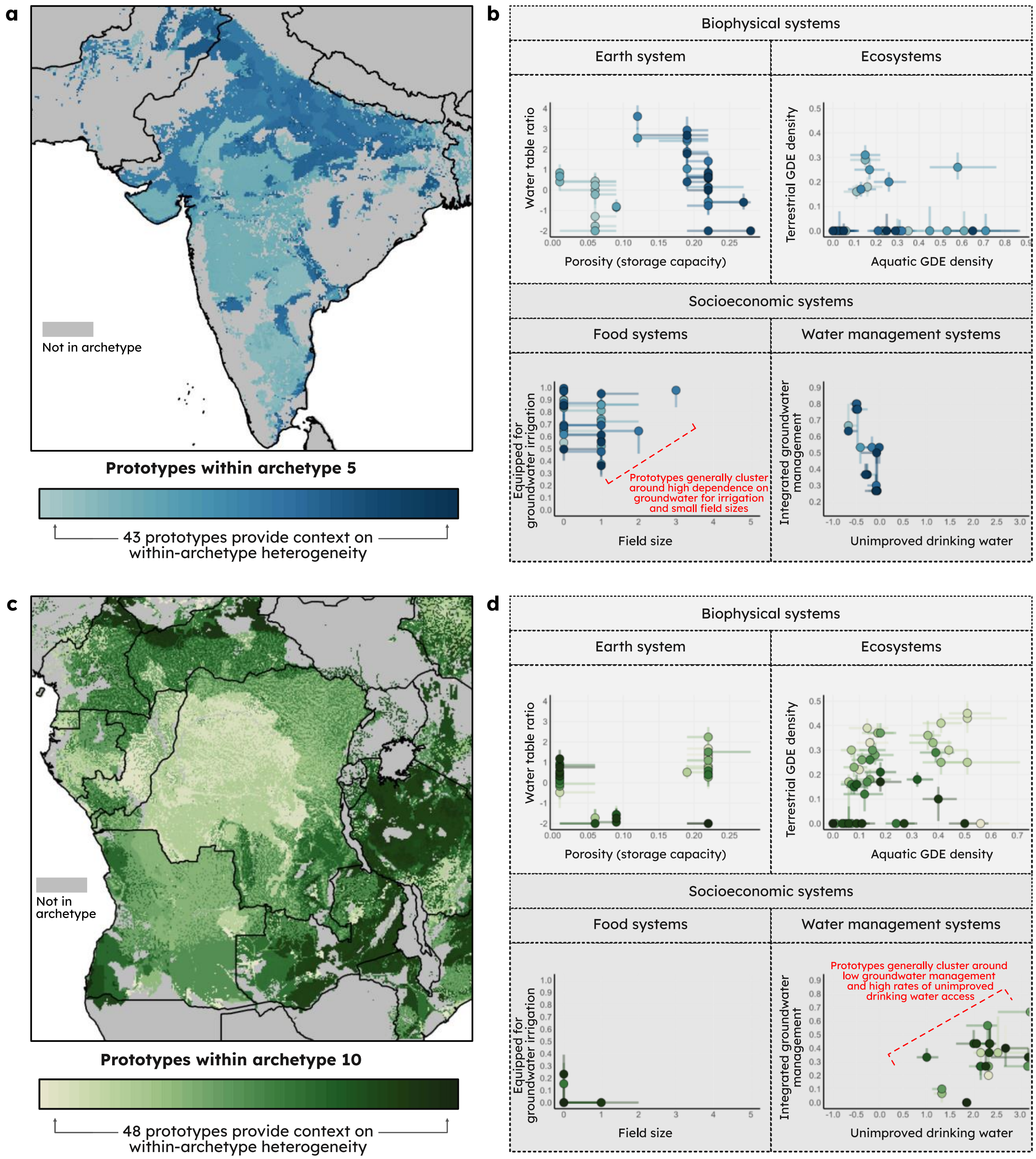

598 **Figure 10: Prototype distributions within selected archetypes. (a) Map of prototypes within GA5**
599 **for the Indian subcontinent. (b) Distribution of groundwater functions across the 43 prototypes**
600 **that together comprise GA5. (c) Map of prototypes within GA10 for the Congo Basin and**

surrounding regions. (d) Distribution of groundwater functions across the 48 prototypes that together comprise GA10.

For both regions, the prototypes that are distributed within these archetypes also show spatially contiguous patterns (Figure 10a, Figure 10c). Investigating the distribution of functions within prototypes (Figure 10b and 10d) show that while prototypes within a given archetype are closely clustered within the functions which characterise the archetype, there remains considerable heterogeneity across the prototypes' other functions. For example, prototypes within GA5 are similar in their food system functions but show variation across their Earth system, ecosystem, and water management system functions (Figure 10b). These variations were not sufficient to warrant the prototype being classified within a different or new archetype in our methodology, but provide greater transparency regarding groundwater system function variation within the simplified archetypes.

<u>3.5 Archetype uncertainty and robustness</u>

As the archetypes were derived on a sample of the input data, we tested the robustness of our archetyping results to the sampling procedure by repeating the archetype derivation procedure on five alternate samples (Text S4). We found an average total uncertainty of 8% between the original archetypes map and the alternative archetype maps produced. This means that the archetype relationship between ~92% of any two randomly sampled points was preserved in the alternate archetype maps (i.e., two points with matching archetypes also have matching archetypes in the alternative archetype map, or two points with non-matching archetypes also have non-matching archetypes in the alternative archetype map). Total uncertainty varies for individual archetypes and we found GA5, GA6, and GA7 to have the lowest total uncertainties at 2% each, while GA1 had the largest total uncertainty at 15%. In fact, only GA1, GA2, and GA4 had total uncertainties greater than the average total uncertainty of 8%. There is an inverse relationship between this robustness analysis and the residual distributions within archetypes (Figure 9). That is, archetypes with larger residual distributions tend to have lower total uncertainty, meaning the archetype is more regularly reproduced in alternative archetype iterations, and vice versa. Thus, the combination of these two exercises provides insight regarding the robustness of individual archetypes (i.e., GA5, GA6, GA7 as quite robust, and GA1 and GA2 as less robust). We additionally deconstruct total uncertainty into the components of matching uncertainty and differentiation uncertainty, which are described and reported on in Text S4.

3.6 A step towards characterising global groundwater-connected systems

These archetypes offer a plausible and robustly derived but not definitive set of groundwater system types. This limitation stems from the underlying nature of archetypes as conceptual constructs (Oberlack et al. 2019) rather than physical entities (one cannot head to the field and measure the presence or absence of an archetype). That is, archetypes correspond to specific research questions and their associated conceptual model. The archetypes we have derived represent clearly discernible empirical regularities in groundwater's large-scale socioeconomic, ecological, and Earth system functions but archetypes can likewise be constructed for other system conceptualisations and often target specific phenomena of interest (cf. Oberlack et al. 2019). Thus, as the first archetyping analysis for groundwater systems globally, the presented archetypes offer a generalised, baseline system typology from which more specific or targeted archetypes and their applications can be developed.

In this sense, the presented archetypes and the archetyping approach more broadly, can serve as a useful starting point to guide theory development on dynamic groundwater-connected system behaviour at the global scale. Future groundwater archetypes, given adequate data availability, could include a temporal dynamic, such as how archetype membership changes over time. Such temporally dynamic archetyping approaches are particularly necessary to test dynamic cause-effect relationships, develop indicators of social-ecological system resilience, and develop middle-range theories of change in these deeply intertwined, diverse systems.

Middle-range theories are “contextual generalisations that describe chains of causal mechanisms explaining a well-bounded range of phenomena, as well as the conditions that trigger, enable, or prevent these causal chains” (Meyfroidt et al. 2018). Archetypes, appropriately constructed, provide necessary conditions for this theory development. For instance, archetypes can serve as otherwise comparable units for testing effects of specific policies or interventions to generate bounded sets of conditions that can be linked to particular system behaviours (Eisenack et al. 2021). It is our view that there is a lack of such middle-range theories for large-scale groundwater systems, and generalising relationships in deeply intertwined social-ecological systems to large-scales has proven a challenge in recent freshwater studies (for example, biodiversity responses to environmental flow transgressions) (Mohan et al. 2022).

The archetypes can also serve an important purpose of provoking debate, community discussions, and future work on approaches that conceptualise, represent, and classify groundwater systems. For instance, many physical aquifer properties are not included explicitly in our study such as hydraulic conductivity, streambed conductance, or recharge. Our decision to exclude these properties stemmed from our focus on groundwater's large-scale functions and we view these physical system properties to be implicitly represented through their impact on various functions (e.g., recharge and hydraulic conductivity contribute to the water table ratio). Yet, it is possible that these are important omissions for other hydrogeologists. On this basis, we view debate and alternative system typologies as healthy and enriching developments of a growing focus on groundwater archetyping.

3.7 Archetype validity

As conceptual constructs, archetype validation is characteristically different than traditional validation procedures. Recognising this amid a lack of formal validation procedures across the existing archetyping literature, Piemontese et al. (2022) proposed six dimensions for qualitative evaluation of archetype validity. These dimensions are: conceptual validity (the strength of the conceptual research framing), construct validity (representativeness of the selected variables), internal validity (appropriateness of method), external validity (clearly stated boundaries of study design), empirical validity (correspondence with documented outcomes), and application validity (usefulness for final knowledge users). It is challenging to strongly address all six validity dimensions in a given study as there are often trade-offs between validity dimensions. Thus, these dimensions are not a necessary set of standards that must be met in every study but rather a qualitative framework to contextualise the contribution and limitations of any individual archetyping study (Piemontese et al. 2022).

We evaluate our study as having strong construct and internal validity, moderate conceptual and external validity, and weak empirical and application validity. From a construct and internal validity perspective, our study is based on documented and widespread groundwater functions, is guided by a clearly defined research question, and applied a leading, robust, and reproducible derivation methodology. From a conceptual validity perspective, we acknowledge the social-ecological system archetyping performed is conceptually broad in contrast to conventional archetyping studies which focus on specific, target phenomenon for a given jurisdiction and we view our approach to quantify archetype uncertainty as a partial treatment of external validity. We did not address the other dimensions of archetype validity, which could require or benefit from alternative methodologies including engagement with potential archetype users.

3.8 Data limitations as future opportunities

Our extensive collection and analysis of global datasets documenting groundwater's socioeconomic, ecological, and Earth system functions serves a secondary purpose as an applied assessment and mirror of current data availability on global groundwater functions. While sufficient data were available to conduct this study, clear data limitations include temporal mismatch across datasets and a lack of time series data. For groundwater archetyping to realise its full potential, it is critical for global datasets to be periodically and reliably updated to enable temporal analysis, and to expand to encompass a wider range of groundwater-connected systems. Such datasets for future development and inclusion in archetyping could include groundwater use for industrial, mining, energy generation, or manufacturing purposes, groundwater's biogeochemical functions, ecosystem services of groundwater-dependent ecosystems, and the cultural values of groundwater. Expanding global groundwater datasets to include these system connections with groundwater could facilitate the development of more nuanced archetypes of groundwater systems that could be more suitable for integration with bottom-up approaches to study and manage groundwater systems (e.g., Zwarteveen et al. 2021).

4 Conclusion

A set of 10 global groundwater archetypes were derived based on groundwater's large-scale socioeconomic, ecological, and Earth system functions using a two-stage self-organising map methodology. To our knowledge, this study represents the first application of archetype analysis to the global groundwater literature, and it also represents the first application of the two-stage self-organising map methodology in the archetyping literature. The derived archetypes represent unique configurations of groundwater functions that reoccur over broad spatial extents, and represent a new lens through which to view, study, and manage global groundwater resources. We find each of the 37 large aquifer systems of the world are characterised by multiple archetypes, highlighting the heterogeneity of system types and functions within these large aquifers and the need for better representation of this functional heterogeneity in global-scale studies. These archetypes represent a plausible and robustly derived set of baseline archetypes in hopes of stimulating community discussions on their utility and to facilitate future work that continues to build on the archetyping concept and its applications to complex groundwater dynamics in social-ecological systems.

Open research

All analyses were conducted using the R project for statistical computing (R Core Team, 2023), using the R packages *kohonen* (Wehrens and Kruisselbrink 2018) and *aweSOM* (Boelaert et al. 2022) to develop and evaluate self-organising maps (SOMs). Landscape metrics of the archetypes within the large aquifer systems of the world were computed using the *landscapemetrics* package (Hesselbarth et al. 2019). Scripts developed to produce all results in this study are available at https://github.com/XanderHuggins/gcs-archetypes. Archetype data will be deposited on Borealis (https://borealisdata.ca/), the Canadian Dataverse Repository, upon manuscript acceptance.

Acknowledgements

X.H. was supported by an Alexander Graham Bell Canada Graduate Scholarship from the Natural Sciences and Engineering Research Council (NSERC) of Canada. X.H. also conducted early-stages of this study while participating in the Young Scientists Summer Programme (YSSP) at the International Institute for Applied Systems Analysis and would like to thank Taher Kahil and Amanda Palazzo for their mentorship during this program. The authors also would like to thank Dor Fridman, Vili Virkki and Ingo Fetzer for feedback on early versions of the manuscript.

Conflict of interest

The authors declare no conflicts of interest.

References

Abbott, B. W., K. Bishop, J. P. Zarnetske, C. Minaudo, F. S. Chapin, S. Krause, D. M. Hannah, et al. (2019). Human domination of the global water cycle absent from depictions and perceptions. *Nature Geoscience* 12, no. 7: 533–40, https://doi.org/10.1038/s41561-019-0374-y.

Aeschbach-Hertig, W., and T. Gleeson. (2012). Regional strategies for the accelerating global problem of groundwater depletion. *Nature Geoscience* 5, no. 12: 853–61, https://doi.org/10.1038/ngeo1617.

Beckmann, M., G. Didenko, J. M. Bullock, A. F. Cord, A. Paulus, G. Ziv, and T. Václavík. (2022). Archetypes of agri-environmental potential: a multi-scale typology for spatial stratification and upscaling in Europe. *Environmental Research Letters* 17, no. 11: 115008, https://doi.org/10.1088/1748-9326/ac9cf5.

Berkes, F., and C. Folke. (1998). *Linking Social and Ecological Systems: Management Practices and Social Mechanisms for Building Resilience*. Cambridge University Press.

Boelaert, J., E. Ollion, J. Sodoge, M. Megdoud, O. Naji, A. L. Kote, T. Renoud, and S. Hym. (2022). aweSOM: Interactive Self-Organizing Maps, https://cran.r-project.org/package=aweSOM.

Buchadas, A., M. Baumann, P. Meyfroidt, and T. Kuemmerle. (2022). Uncovering major types of deforestation frontiers across the world's tropical dry woodlands. *Nature Sustainability* 5, no. 7: 619–27, https://doi.org/10.1038/s41893-022-00886-9.

Condon, L. E., K. H. Markovich, C. A. Kelleher, J. J. McDonnell, G. Ferguson, and J. C. McIntosh. (2020). Where Is the Bottom of a Watershed? *Water Resources Research* 56, no. 3: e2019WR026010, https://doi.org/10.1029/2019WR026010.

Curran, D., T. Gleeson, and X. Huggins. (2023). Applying a science-forward approach to groundwater regulatory design. *Hydrogeology Journal* 31, no. 4: 853–71, https://doi.org/10.1007/s10040-023-02625-6.

Cuthbert, M. O., T. Gleeson, N. Moosdorf, K. M. Befus, A. Schneider, J. Hartmann, and B. Lehner. (2019). Global patterns and dynamics of climate–groundwater interactions. *Nature Climate Change* 9, no. 2: 137–41, https://doi.org/10.1038/s41558-018-0386-4.

Dalin, C., Y. Wada, T. Kastner, and M. J. Puma. (2017). Groundwater depletion embedded in international food trade. *Nature* 543, no. 7647: 700–704, https://doi.org/10.1038/nature21403.

Delgado, S., C. Higuera, J. Calle-Espinosa, F. Morán, and F. Montero. (2017). A SOM prototype-based cluster analysis methodology. *Expert Systems with Applications* 88, December: 14–28, https://doi.org/10.1016/j.eswa.2017.06.022.

Döll, P., and K. Fiedler. (2008). Global-scale modeling of groundwater recharge. *Hydrology and Earth System Sciences* 12, no. 3: 863–85, https://doi.org/10.5194/hess-12-863-2008.

Döll, P., H. Müller Schmied, C. Schuh, F. T. Portmann, and A. Eicker. (2014). Global-scale assessment of groundwater depletion and related groundwater abstractions: Combining hydrological modeling with information from well observations and GRACE satellites. *Water Resources Research* 50, no. 7: 5698–5720, https://doi.org/10.1002/2014WR015595.

Dormann, C. F., J. Elith, S. Bacher, C. Buchmann, G. Carl, G. Carré, J. R. G. Marquéz, et al. (2013). Collinearity: a review of methods to deal with it and a simulation study evaluating their performance. *Ecography* 36, no. 1: 27–46, https://doi.org/10.1111/j.1600-0587.2012.07348.x.

Eisenack, K., C. Oberlack, and D. Sietz. (2021). Avenues of archetype analysis: roots, achievements, and next steps in sustainability research. *Ecology and Society* 26, no. 2, https://doi.org/10.5751/ES-12484-260231.

Ellis, E. C., and N. Ramankutty. (2008). Putting people in the map: anthropogenic biomes of the world. *Frontiers in Ecology and the Environment* 6, no. 8: 439–47, https://doi.org/10.1890/070062.

Famiglietti, J. S. (2014). The global groundwater crisis. *Nature Climate Change* 4, no. 11: 945–48, https://doi.org/10.1038/nclimate2425.

Fan, Y., G. Miguez-Macho, E. G. Jobbágy, R. B. Jackson, and C. Otero-Casal. (2017). Hydrologic regulation of plant rooting depth. *Proceedings of the National Academy of Sciences* 114, no. 40: 10572–77, https://doi.org/10.1073/pnas.1712381114.

Ferguson, G., J. C. McIntosh, O. Warr, B. Sherwood Lollar, C. J. Ballentine, J. S. Famiglietti, J.-H. Kim, et al. (2021). Crustal Groundwater Volumes Greater Than Previously Thought. *Geophysical Research Letters* 48, no. 16: e2021GL093549, https://doi.org/10.1029/2021GL093549.

Foster, S., and P. Chilton. (2003). Groundwater: the processes and global significance of aquifer degradation. *Philosophical Transactions of the Royal Society of London. Series B: Biological Sciences* 358, no. 1440: 1957–72, https://doi.org/10.1098/rstb.2003.1380.

Foster, Stephen, J. Chilton, G.-J. Nijsten, and A. Richts. (2013). Groundwater—a global focus on the “local resource.” *Current Opinion in Environmental Sustainability* 5, no. 6: 685–95, https://doi.org/10.1016/j.cosust.2013.10.010.

Fridman, D., T. Koellner, and M. Kissinger. (2021). Exploring global interregional food system’s sustainability using the functional regions typology. *Global Environmental Change* 68, May: 102276, https://doi.org/10.1016/j.gloenvcha.2021.102276.

Giordano, M., and K. G. Villholth, eds. (2007). *The agricultural groundwater revolution: opportunities and threats to development*. Comprehensive Assessment of Water Management in Agriculture 3. Wallingford, UK: CAB International, https://cgspace.cgiar.org/handle/10568/36474.

Gleeson, T, M. Cuthbert, G. Ferguson, and D. Perrone. (2020). Global Groundwater Sustainability, Resources, and Systems in the Anthropocene. *Annual Review of Earth and Planetary Sciences* 48, no. 1: 431–63, https://doi.org/10.1146/annurev-earth-071719-055251.

Gleeson, T, X. Huggins, R. Connor, P. Arrojo-Agudo, and E. Vázquez Suñé. (2022). Groundwater and ecosystems. In *The United Nations World Water Development Report 2022: groundwater: making the invisible visible*, 89–100. Paris, France: UNESCO World Water Assessment Programme, https://unesdoc.unesco.org/ark:/48223/pf0000380721.

Gleeson, T., N. Moosdorf, J. Hartmann, and L. P. H. van Beek. (2014). A glimpse beneath earth’s surface: GLobal HYdrogeology MaPS (GLHYMPS) of permeability and porosity. *Geophysical Research Letters* 41, no. 11: 3891–98, https://doi.org/10.1002/2014GL059856.

Gleeson, T, L. Wang-Erlandsson, M. Porkka, S. C. Zipper, F. Jaramillo, D. Gerten, I. Fetzer, et al. (2020). Illuminating water cycle modifications and Earth system resilience in the Anthropocene. *Water Resources Research* 56, no. 4: e2019WR024957, https://doi.org/10.1029/2019WR024957.

Gleeson, T., K. M. Befus, S. Jasechko, E. Luijendijk, and M. B. Cardenas. (2016). The global volume and distribution of modern groundwater. *Nature Geoscience* 9, no. 2: 161–67, https://doi.org/10.1038/ngeo2590.

Graaf, I. E. M. de, T. Gleeson, L. P. H. (Rens) van Beek, E. H. Sutanudjaja, and M. F. P. Bierkens. (2019). Environmental flow limits to global groundwater pumping. *Nature* 574, no. 7776: 90–94, https://doi.org/10.1038/s41586-019-1594-4.

Graesser, J., and N. Ramankutty. (2017). Detection of cropland field parcels from Landsat imagery. *Remote Sensing of Environment* 201, November: 165–80, https://doi.org/10.1016/j.rse.2017.08.027.

Haitjema, H. M., and S. Mitchell-Bruker. (2005). Are Water Tables a Subdued Replica of the Topography? *Groundwater* 43, no. 6: 781–86, https://doi.org/10.1111/j.1745-6584.2005.00090.x.

Herrera-García, G., P. Ezquerro, R. Tomás, M. Béjar-Pizarro, J. López-Vinielles, M. Rossi, R. M. Mateos, et al. (2021). Mapping the global threat of land subsidence. *Science* 371, no. 6524: 34–36, https://doi.org/10.1126/science.abb8549.

Herrero, M., P. K. Thornton, B. Power, J. R. Bogard, R. Remans, S. Fritz, J. S. Gerber, et al. (2017). Farming and the geography of nutrient production for human use: a transdisciplinary analysis. *The Lancet Planetary Health* 1, no. 1: e33–42, https://doi.org/10.1016/S2542-5196(17)30007-4.

Hesselbarth, M. H. K., M. Sciaini, K. A. With, K. Wiegand, and J. Nowosad. (2019). landscapemetrics: an open-source R tool to calculate landscape metrics. *Ecography* 42, no. 10: 1648–57, https://doi.org/10.1111/ecog.04617.

Huggins, X., T. Gleeson, J. Castilla-Rho, C. Holley, V. Re, and J. S. Famiglietti. (2023). Groundwater Connections and Sustainability in Social-Ecological Systems. *Groundwater* 61, no. 4: 463–78, https://doi.org/10.1111/gwat.13305.

Huggins, X., T. Gleeson, M. Kummu, S. C. Zipper, Y. Wada, T. J. Troy, and J. S. Famiglietti. (2022). Hotspots for social and ecological impacts from freshwater stress and storage loss. *Nature Communications* 13, no.1:439, https://doi.org/10.1038/s41467-022-28029-w.

Huggins, X., T. Gleeson, D. Serrano, S. Zipper, F. Jehn, M. M. Rohde, R. Abell, K. Vigerstol, and A. Hartmann. (2023). Overlooked risks and opportunities in groundwatersheds of the world's protected areas. *Nature Sustainability* 6, no. 7: 855–64, https://doi.org/10.1038/s41893-023-01086-9.

Jasechko, S., and D. Perrone. (2021). Global groundwater wells at risk of running dry. *Science* 372, no. 6540: 418–21, https://doi.org/10.1126/science.abc2755.

Jehn, F. U., K. Bestian, L. Breuer, P. Kraft, and T. Houska. (2020). Using hydrological and climatic catchment clusters to explore drivers of catchment behavior. *Hydrology and Earth System Sciences* 24, no. 3: 1081–1100, https://doi.org/10.5194/hess-24-1081-2020.

Kaufmann, D., A. Kraay, and M. Mastruzzi. (2011). The Worldwide Governance Indicators: Methodology and Analytical Issues. *Hague Journal on the Rule of Law* 3, no. 2: 220–46, https://doi.org/10.1017/S1876404511200046.

Kløve, B., P. Ala-aho, G. Bertrand, Z. Boukalova, A. Ertürk, N. Goldscheider, J. Ilmonen, et al. (2011). Groundwater dependent ecosystems. Part I: Hydroecological status and trends. *Environmental Science & Policy*, Adapting to Climate Change: Reducing Water-related Risks in Europe, 14, no. 7: 770–81, https://doi.org/10.1016/j.envsci.2011.04.002.

Kohonen, T. (2001). *Self-Organizing Maps*. Vol. 30. Springer Series in Information Sciences. Berlin, Heidelberg: Springer, https://doi.org/10.1007/978-3-642-56927-2.

Kok, M., M. Lüdeke, P. Lucas, T. Sterzel, C. Walther, P. Janssen, D. Sietz, and I. de Soysa. (2016). A new method for analysing socio-ecological patterns of vulnerability. *Regional Environmental Change* 16, no. 1: 229–43, https://doi.org/10.1007/s10113-014-0746-1.

Konikow, L. F. (2011). Contribution of global groundwater depletion since 1900 to sea-level rise. *Geophysical Research Letters* 38, no. 17, https://doi.org/10.1029/2011GL048604.

Kuzma, S., M. Bierkens, S. Lakshman, T. Luo, L. Saccoccia, E. Sutanudjaja, and R. van Beek. (2023). Aqueduct 4.0: Updated decision-relevant global water risk indicators. Technical Note, https://doi.org/10.46830/writn.23.00061.

Lall, U., L. Josset, and T. Russo. (2020). A Snapshot of the World's Groundwater Challenges. *Annual Review of Environment and Resources* 45, no. 1: 171–94, https://doi.org/10.1146/annurev-environ-102017-025800.

Lesiv, M., J. C. Laso Bayas, L. See, M. Duerauer, D. Dahlia, N. Durando, R. Hazarika, et al. (2019). Estimating the global distribution of field size using crowdsourcing. *Global Change Biology* 25, no. 1: 174–86, https://doi.org/10.1111/gcb.14492.

Margat, J. (2008). *Les Eaux souterraines dans le monde*. Paris, France: UNESCO, https://unesdoc.unesco.org/ark:/48223/pf0000162188.

Maxwell, R. M., and S. J. Kollet. (2008). Interdependence of groundwater dynamics and land-energy feedbacks under climate change. *Nature Geoscience* 1, no. 10: 665–69, https://doi.org/10.1038/ngeo315.

Meyfroidt, P., R. Roy Chowdhury, A. de Bremond, E. C. Ellis, K.-H. Erb, T. Filatova, R. D. Garrett, et al. (2018). Middle-range theories of land system change. *Global Environmental Change* 53, November: 52–67, https://doi.org/10.1016/j.gloenvcha.2018.08.006.

Meyfroidt, P. (2017). Mapping farm size globally: benchmarking the smallholders debate. *Environmental Research Letters* 12, no. 3: 031002, https://doi.org/10.1088/1748-9326/aa5ef6.

Meyfroidt, P., A. de Bremond, C. M. Ryan, E. Archer, R. Aspinall, A. Chhabra, G. Camara, et al. (2022). Ten facts about land systems for sustainability. *Proceedings of the National Academy of Sciences* 119, no. 7: e2109217118, https://doi.org/10.1073/pnas.2109217118.

Mohan, C., T. Gleeson, J. S. Famiglietti, V. Virkki, M. Kummu, M. Porkka, L. Wang-Erlandsson, X. Huggins, D. Gerten, and S. C. Jähnig. (2022). Poor correlation between large-scale environmental flow violations and freshwater biodiversity: implications for water resource management and the freshwater planetary boundary. *Hydrology and Earth System Sciences* 26, no. 23: 6247–62, https://doi.org/10.5194/hess-26-6247-2022.

Mukherji, A., and T. Shah. (2005). Groundwater socio-ecology and governance: a review of institutions and policies in selected countries. *Hydrogeology Journal* 13, no. 1: 328–45, https://doi.org/10.1007/s10040-005-0434-9.

Neudert, R., A. Salzer, N. Allahverdiyeva, J. Etzold, and V. Beckmann. (2019). Archetypes of common village pasture problems in the South Caucasus: insights from comparative case studies in Georgia and Azerbaijan. *Ecology and Society* 24, no. 3, https://doi.org/10.5751/ES-10921-240305.

Nowosad, J., and T. F. Stepinski. (2019). Information theory as a consistent framework for quantification and classification of landscape patterns. *Landscape Ecology* 34, no. 9: 2091–2101, https://doi.org/10.1007/s10980-019-00830-x.

Oberlack, C., S. Pedde, L. Piemontese, T. Václavík, and D. Sietz. (2023). Archetypes in support of tailoring land-use policies. *Environmental Research Letters* 18, no. 6: 060202, https://doi.org/10.1088/1748-9326/acd802.

Oberlack, C., D. Sietz, E. Bürgi Bonanomi, A. de Bremond, J. Dell'Angelo, K. Eisenack, E. Ellis, et al. (2019). Archetype analysis in sustainability research: meanings, motivations, and evidence-based policy making. *Ecology and Society* 24, no. 2, https://doi.org/10.5751/ES-10747-240226.

Ostrom, E. (2009). A General Framework for Analyzing Sustainability of Social-Ecological Systems. *Science* 325, no. 5939: 419–22, https://doi.org/10.1126/science.1172133.

Pacheco-Romero, M., M. Vallejos, J. M. Paruelo, D. Alcaraz-Segura, M. T. Torres-García, M. J. Salinas-Bonillo, and J. Cabello. (2022). A data-driven methodological routine to identify key indicators for social-ecological system archetype mapping. *Environmental Research Letters* 17, no. 4: 045019, https://doi.org/10.1088/1748-9326/ac5ded.

Piemontese, L., R. Neudert, C. Oberlack, S. Pedde, M. Roggero, A. Buchadas, D. A. Martin, et al. (2022). Validity and validation in archetype analysis: practical assessment framework and guidelines. *Environmental Research Letters* 17, no. 2: 025010, https://doi.org/10.1088/1748-9326/ac4f12.

R Core Team. (2023). R: a language and environment for statistical computing. Version 4.3.1. https://www.r-project.org/.
Reinecke, R., L. Foglia, S. Mehl, J. D. Herman, A. Wachholz, T. Trautmann, and P. Döll. (2019). Spatially distributed sensitivity of simulated global groundwater heads and flows to hydraulic conductivity, groundwater recharge, and surface water body parameterization. *Hydrology and Earth System Sciences* 23, no. 11: 4561–82, https://doi.org/10.5194/hess-23-4561-2019.
Ricciardi, V., N. Ramankutty, Z. Mehrabi, L. Jarvis, and B. Chookolingo. (2018). How much of the world's food do smallholders produce? *Global Food Security* 17, June: 64–72, https://doi.org/10.1016/j.gfs.2018.05.002.
Richts, A., W. F. Struckmeier, and M. Zaepke. (2011). WHYMAP and the Groundwater Resources Map of the World 1:25,000,000. In *Sustaining Groundwater Resources: A Critical Element in the Global Water Crisis*, edited by J. A. A. Jones, 159–73. International Year of Planet Earth. Dordrecht: Springer Netherlands, https://doi.org/10.1007/978-90-481-3426-7_10.
Riitters, K. H., R. V. O'Neill, J. D. Wickham, and K. B. Jones. (1996). A note on contagion indices for landscape analysis. *Landscape Ecology* 11, no. 4: 197–202, https://doi.org/10.1007/BF02071810.
Rocha, J., K. Malmborg, L. Gordon, K. Brauman, and F. DeClerck. (2020). Mapping social-ecological systems archetypes. *Environmental Research Letters* 15, no. 3: 034017, https://doi.org/10.1088/1748-9326/ab666e.
Rohde, M. M., R. Froend, and J. Howard. (2017). A Global Synthesis of Managing Groundwater Dependent Ecosystems Under Sustainable Groundwater Policy. *Groundwater* 55, no. 3: 293–301, https://doi.org/10.1111/gwat.12511.
Saito, L., B. Christian, J. Diffley, H. Richter, M. M. Rohde, and S. A. Morrison. (2021). Managing Groundwater to Ensure Ecosystem Function. *Groundwater* 59, no. 3: 322–33, https://doi.org/10.1111/gwat.13089.
Scanlon, B. R., S. Fakhreddine, A. Rateb, I. de Graaf, J. Famiglietti, T. Gleeson, R. Q. Grafton, et al. (2023). Global water resources and the role of groundwater in a resilient water future. *Nature Reviews Earth & Environment* 4, no. 2: 87–101, https://doi.org/10.1038/s43017-022-00378-6.
Shah, T., J. Burke, and K. Villholth. (2007). Groundwater: A global assessment of scale and significance, in Water for Food, Water for Life, edited by D. Molden, pp. 395–423, Earthscan, London, U. K.
Siebert, S., J. Burke, J. M. Faures, K. Frenken, J. Hoogeveen, P. Döll, and F. T. Portmann. (2010). Groundwater use for irrigation – a global inventory. *Hydrology and Earth System Sciences* 14, no. 10: 1863–80, https://doi.org/10.5194/hess-14-1863-2010.
Sietz, D., U. Frey, M. Roggero, Y. Gong, N. Magliocca, R. Tan, P. Janssen, and T. Václavík. (2019). Archetype analysis in sustainability research: methodological portfolio and analytical frontiers. *Ecology and Society* 24, no. 3, https://doi.org/10.5751/ES-11103-240334.
Sietz, D., M. K. B. Lüdeke, and C. Walther. (2011). Categorisation of typical vulnerability patterns in global drylands. *Global Environmental Change*, Special Issue on The Politics and Policy of Carbon Capture and Storage, 21, no. 2: 431–40, https://doi.org/10.1016/j.gloenvcha.2010.11.005.
Sietz, D., and R. Neudert. (2022). Taking stock of and advancing knowledge on interaction archetypes at the nexus between land, biodiversity, food and climate. *Environmental Research Letters* 17, no. 11: 113004, https://doi.org/10.1088/1748-9326/ac9a5c.
Simpson, E. H. (1949). Measurement of Diversity. *Nature* 163, no. 4148: 688–688, https://doi.org/10.1038/163688a0.

Sivapalan, M., M. Konar, V. Srinivasan, A. Chhatre, A. Wutich, C. A. Scott, J. L. Wescoat, and I. Rodríguez-Iturbe. (2014). Socio-hydrology: Use-inspired water sustainability science for the Anthropocene. *Earth's Future* 2, no. 4: 225–30, https://doi.org/10.1002/2013EF000164.

Taylor, R. G., B. Scanlon, P. Döll, M. Rodell, R. van Beek, Y. Wada, L. Longuevergne, et al. (2013). Ground water and climate change. *Nature Climate Change* 3, no. 4: 322–29, https://doi.org/10.1038/nclimate1744.

UNEP. (2021). *Progress on Integrated Water Resources Management. SDG 6 Series: Global Indicator 6.5.1 Updates and Acceleration Needs*, http://iwrmdataportal.unepdhi.org/publications/global.

Václavík, T., S. Lautenbach, T. Kuemmerle, and R. Seppelt. (2013). Mapping global land system archetypes. *Global Environmental Change* 23, no. 6: 1637–47, https://doi.org/10.1016/j.gloenvcha.2013.09.004.

Van Lanen, H. a. J., N. Wanders, L. M. Tallaksen, and A. F. Van Loon. (2013). Hydrological drought across the world: impact of climate and physical catchment structure. *Hydrology and Earth System Sciences* 17, no. 5: 1715–32, https://doi.org/10.5194/hess-17-1715-2013.

Varis, O., M. Taka, and M. Kummu. (2019). The Planet's Stressed River Basins: Too Much Pressure or Too Little Adaptive Capacity? *Earth's Future* 7, no. 10: 1118–35, https://doi.org/10.1029/2019EF001239.

Varshney, L. R., and J. Z. Sun. (2013). Why do we perceive logarithmically? *Significance* 10, no. 1: 28–31, https://doi.org/10.1111/j.1740-9713.2013.00636.x.

Vesanto, J., and E. Alhoniemi. (2000). Clustering of the self-organizing map. *IEEE Transactions on Neural Networks* 11, no. 3: 586–600, https://doi.org/10.1109/72.846731.

Villholth, K. G., and K. Conti. (2018). Groundwater governance: rationale, definition, current state and heuristic framework. In *Advances in groundwater governance*, edited by K. G. Villholth, E. López-Gunn, A. Garrido, J. A. M. van der Gun, and K. I. Conti. Leiden, The Netherlands: CRC Press/Balkema.

Wada, Y., L. P. H. van Beek, and M. F. P. Bierkens. (2012). Nonsustainable groundwater sustaining irrigation: A global assessment. *Water Resources Research* 48, no. 6, https://doi.org/10.1029/2011WR010562.

Wehrens, R., and J. Kruisselbrink. (2018). Flexible Self-Organizing Maps in kohonen 3.0. *Journal of Statistical Software* 87, November: 1–18, https://doi.org/10.18637/jss.v087.i07.

Wessel, P., J. F. Luis, L. Uieda, R. Scharroo, F. Wobbe, W. H. F. Smith, and D. Tian. (2019). The Generic Mapping Tools Version 6. *Geochemistry, Geophysics, Geosystems* 20, no. 11: 5556–64, https://doi.org/10.1029/2019GC008515.

Wessel, P., and W. H. F. Smith. (1996). A global, self-consistent, hierarchical, high-resolution shoreline database. *Journal of Geophysical Research: Solid Earth* 101, no. B4: 8741–43, https://doi.org/10.1029/96JB00104.

Wierzchoń, S., and M. Kłopotek. (2018). *Modern Algorithms of Cluster Analysis*. Vol. 34. Studies in Big Data. Cham: Springer International Publishing, https://doi.org/10.1007/978-3-319-69308-8.

Winkler, K., R. Fuchs, M. Rounsevell, and M. Herold. (2021). Global land use changes are four times greater than previously estimated. *Nature Communications* 12, no. 1: 2501, https://doi.org/10.1038/s41467-021-22702-2.

Winter, T. (2001). The Concept of Hydrologic Landscapes. *Journal of the American Water Resources Association* 37, no. 2: 335–49, https://doi.org/10.1111/j.1752-1688.2001.tb00973.x.

World Bank. (2023). Worldwide Governance Indicators, https://info.worldbank.org/governance/wgi/. Last accessed 22 August 2023.

Zanden, E. H. van der, C. Levers, P. H. Verburg, and T. Kuemmerle. (2016). Representing composition, spatial structure and management intensity of European agricultural landscapes: A new typology. *Landscape and Urban Planning* 150, June: 36–49, https://doi.org/10.1016/j.landurbplan.2016.02.005.

Zwarteveen, M., M. Kuper, C. Olmos-Herrera, M. Dajani, J. Kemerink-Seyoum, C. Frances, L. Beckett, et al. (2021). Transformations to groundwater sustainability: from individuals and pumps to communities and aquifers. *Current Opinion in Environmental Sustainability* 49, April: 88–97, https://doi.org/10.1016/j.cosust.2021.03.004.